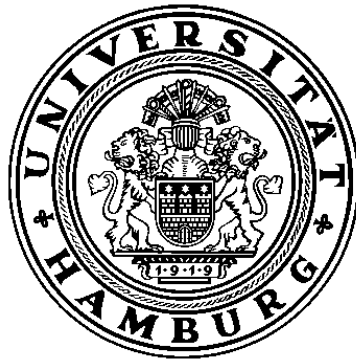


Capability to detect and categorise real and
hypothetical atmospheric concentrations of
radioxenon for Comprehensive Nuclear-
Test-Ban Treaty verification

Frederik Postelt



- *Diploma Thesis* -

Department of Physics
University of Hamburg

written at the

**Carl Friedrich von Weizsäcker Centre for Science and Peace
Research of the University of Hamburg (ZNF),**

the

**Provisional Technical Secretariat (PTS) of the Comprehensive
Nuclear-Test-Ban Treaty Organisation (CTBTO), Vienna**

and the

**Department of Physics “Edoardo Amaldi” of the University of
Roma Tre**

under the supervision of

Prof. Dr. Martin B. Kalinowski, ZNF

and as second reviewer

Dr. Paul R. J. Saey, IAEA

Deutscher Titel der Diplomarbeit:

Detektierbarkeit und Kategorisierbarkeit von realen und hypothetischen atmosphärischen Radioxenonkonzentrationen für die Verifikation des Kernwaffenteststopp-Vertrags

I confirm that I have written this thesis completely myself without help other than cited. I agree with the publication of this thesis, subject to CTBTO Preparatory Commission approval. The views expressed herein are those of the author and do not necessarily reflect the views of the CTBTO Preparatory Commission.

Frederik Postelt

Hamburg, 13th July 2012

Abstract

The noble gas xenon has proven to be very useful for the verification regime of the Comprehensive Nuclear-Test-Ban Treaty (CTBT). This is especially true for the detection of underground nuclear explosions and when it comes to the distinction between nuclear and chemical explosions.

In this work a categorisation concept for radioxenon spectra as acquired by the CTBTO is developed further, as well as an algorithm to categorise the spectra without human intervention. The spectra give information about the xenon concentrations in the sampled air and are categorised according to their level of indication that a nuclear test has occurred. To allow a solid categorisation, preconditions are defined, which screen out spectra which are generally not well suited for the algorithm. 25,726 spectra acquired by the CTBTO International Monitoring System (IMS) noble gas network between June 2007 and June 2010 are analysed by acquiring station, xenon isotope and average xenon activity concentration. The categorisation concept is not primarily based on the analysis of absolute concentrations, but on the xenon concentration ratios of the four relevant isotopes Xe-133, Xe-135, Xe-133m and Xe-131m. The xenon ratios Xe-135/Xe-133, Xe-133m/Xe-131m and Xe-133m/Xe-133 are calculated in case of sufficient detections and the first two used for the categorisation. The latter ratio is used as additional information only (as so-called flag). An isotope is detected, if its xenon activity concentration is at least equivalent to the concentration which can just be detected. The so-called Minimum Detectable Concentration (MDC) is calculated for every spectrum for all four relevant xenon isotopes. Non-detected isotopes are substituted by their MDC as long as the other isotope necessary to calculate the according ratio is detected.

The developed algorithm is then tested for its ability to detect nuclear weapon underground tests, which are generally most difficult to detect. Therefore, actual measurements of xenon concentrations released at the Nevada Test Site (NTS) after nuclear underground tests conducted before the finalisation of the CTBT are transferred to the present and their propagation through the atmosphere is simulated with current meteorological fields. The concentrations reaching a defined number of CTBTO noble gas detectors are then added to actual measurements and the arising concentrations are categorised with the algorithm on the basis of xenon ratios.

The presented work supports the concept of using xenon concentration ratios for the categorisation of noble gases, where non-detected xenon concentrations are substituted by the MDC. Furthermore it examines the detectability of historic nuclear weapon underground tests with part of today's International Monitoring System (IMS) based on the developed algorithm.

Zusammenfassung

Das Edelgas Xenon hat sich als sehr nützlich für die Verifikation des Kernwaffenteststopp-Vertrags (englisch Comprehensive Nuclear-Test-Ban Treaty, CTBT) erwiesen. Das gilt besonders für die Entdeckung von unterirdischen Kernwaffentests und für die Unterscheidung zwischen nuklearen und chemischen Explosionen.

In dieser Studie wird ein Kategorisierungskonzept für Radioxenonspektren, wie sie von der CTBTO gemessen werden, weiterentwickelt und ein Algorithmus geschrieben, der diese vollautomatisch durchführt. Die Spektren geben Auskunft über die Xenonkonzentrationen in der untersuchten Luft und werden je nach ihrer Aussagekraft bezüglich nuklearer Tests kategorisiert. Um eine verlässliche Kategorisierung zu ermöglichen werden Vorabbedingungen definiert, die solche Spektren aussortieren, mit denen der Algorithmus tendenziell Probleme hat. 25,726 Spektren, die die CTBTO zwischen Juni 2007 und Juni 2010 aufgenommen hat werden nach aufnehmender Station, Xenonisotop und Xenonaktivitätskonzentration analysiert. Das Kategorisierungskonzept basiert nicht vorrangig auf absoluten Xenonkonzentrationen, sondern auf den Verhältnissen zwischen den vier relevanten Xenonisotopen Xe-133, Xe-135, Xe-133m und Xe-131m. Im Falle von Detektionen der entsprechenden Isotope werden die Verhältnisse Xe-135/Xe-133, Xe-133m/Xe-131m und Xe-133m/Xe-133 gebildet, wobei nur die beiden Ersteren für die Kategorisierung selbst herangezogen werden, während das Letztere nur als zusätzliche Information (als sogenannte flag) angegeben wird. Man spricht von einer Detektion, wenn die Aktivitätskonzentration mindestens der Konzentration entspricht, die gerade noch nachgewiesen werden kann. Diese sogenannte Minimum Detectable Concentration (MDC) wird individuell für jedes Spektrum für alle vier relevanten Xenonisotope berechnet. Nicht detektierte Isotopenkonzentrationen werden durch ihren MDC ersetzt, solange das entsprechende andere Isotop detektiert wurde, das benötigt wird, um das zu bestimmende Verhältnis zu berechnen.

Der entwickelte Algorithmus wird dann auf seine Fähigkeit unterirdische Kernwaffentests zu entdecken getestet, da diese im Allgemeinen am schwersten nachzuweisen sind. Dazu werden echte Xenonmessungen von der Nevada Test Site (NTS) benutzt, die nach unterirdischen Kernwaffentests aufgenommen wurden, bevor der CTBT verhandelt wurde. In der Annahme, dass diese gemessenen Xenonkonzentrationen identisch in der heutigen Zeit freigesetzt werden, wird ihre Ausbreitung in der Atmosphäre mit heutigen meteorologischen Daten simuliert. Die Konzentrationen, die einige bestimmte Edelgasdetektoren der CTBTO erreichen, werden auf die tatsächlich an den entsprechenden Tagen gemessenen aufaddiert und die sich so ergebenden Konzentrationen mit dem entwickelten Algorithmus kategorisiert.

Diese Studie bestätigt das Konzept, Xenonverhältnisse für die Kategorisierung von Edelgasen zu nutzen und dabei nicht detektierte Xenonkonzentrationen durch den MDC zu ersetzen. Desweiteren untersucht sie die Detektierbarkeit von historischen unterirdischen Nuklearwaffentests mit einem Teil des heutigen Überwachungsnetzwerkes (dem International Monitoring System, IMS) mit dem entwickelten Algorithmus.

Contents

Abstract	4
Zusammenfassung	5
List of Figures	7
List of Tables	9
List of Abbreviations	12
1 Introduction	13
2 State of research	15
2.1 Data acquisition	15
2.1.1 Radionuclide technology	17
2.1.1.1 High resolution gamma spectroscopy	19
2.1.1.2 Beta-gamma coincidence measurements	23
2.2 Data processing at the International Data Centre	24
2.2.1 Noble gases	25
2.2.2 State of health criteria	29
2.2.3 Detectability	30
2.2.4 Potential of radioxenon ratios	30
2.3 Radioxenon background	32
2.4 Availability of radioxenon measurement data	32
2.5 Atmospheric transport modelling	33
3 Algorithm validation	35
3.1 Preconditions for categorisation	38
3.2 Rank order	38
3.3 Identification	38
3.4 Abnormal concentration	39
3.5 Isotopic ratios	39
3.6 Source-receptor sensitivity fields and state of health information	40
3.7 Categorisation levels	42
3.8 Results	42

CONTENTS

4	Detectability of historic tests	46
4.1	Nuclear underground test data	46
4.2	Estimation of Xe-131m	47
4.3	Hypothetical International Monitoring System measurements	48
4.4	Calculation of isotopic ratios	50
4.5	Results	51
4.5.1	Absolute contributions of hypothetical tests	53
4.5.2	Source strength variation	53
4.5.3	Detections per station	55
4.5.4	Detection thresholds	56
5	Conclusion and Outlook	60
	References	62
A	Annex	66

List of Figures

2.1	World map with all stations of the International Monitoring System of the CTBTO. [1]	16
2.2	Simplified scheme of a stimulated nuclear fission. [2]	17
2.3	Isobaric decay chains from fission neutron induced fission of Pu-239. [3, 4]	18
2.4	Gamma ray spectrum between 0 and 300 keV. [5]	21
2.5	X-ray-spectrum between 15 and 45 keV. [5]	22
2.6	Beta-gamma detector. [5]	23
2.7	Scheme of the IDC pipeline. [6]	24
2.8	GUI of the high resolution gamma spectra analysis software SAINT2. [5]	26
2.9	GUI of the beta-gamma coincidence spectra analysis software NORFY.	27
2.10	Regions of interest used to analyse beta-gamma coincidence spectra. [7]	28
2.11	Xenon ratio Xe-135/Xe-133 as a function of the ratio Xe-133m/Xe-131m. [8]	31
2.12	Absolute Xe-133 activities for releases at the NTS as a function of time. [9]	33
3.1	GUI of the XE software.	36
3.2	Categorisation concept as applied for the proposed algorithm. [10] . . .	43
4.1	Absolute Xe-133 activities for the 92 releases at the NTS as a function of time.	47
4.2	Frequency distribution of the available IMS measurements at the radionuclide laboratory CAX05 and the IMS stations CAX16, CAX17, DEX33, SEX63, USX74 and USX75 between 17.02.2008 and 21.02.2009.	49
4.3	Plot of the xenon ratios Xe-135/Xe-133 and Xe-133m/Xe-131m. . . .	52
4.4	Plot of the xenon ratios Xe-135/Xe-133 and Xe-133m/Xe-131m.	55
4.5	Xe-133 activities for the amplified releases.	58

LIST OF FIGURES

List of Tables

2.1	Half lives, decay energies and intensities and radiation types of the four relevant radioxenon isotopes and the biggest background emitter lead. [11, 12]	20
2.2	State of health categorisation for samples taken at SPALAX stations. [13]	29
2.3	State of health categorisation for samples taken at SAUNA stations. [14]	29
3.1	Mutual preconditions for the categorisation of spectra from all three station types as applied for the used algorithm.	36
3.2	Preconditions for the categorisation of spectra from SPALAX stations as applied for the used algorithm.	37
3.3	Preconditions for the categorisation of spectra from SAUNA II and ARIX stations as applied for the used algorithm.	37
3.4	Identification code as implemented within the IDC	39
3.5	Categorisation Levels as used by the algorithm.	41
3.6	Parameters used to adapt the categorisation concept and the algorithm.	43
3.7	Overall results from the automatic analysis of 25,726 noble gas spectra acquired by all IMS stations between June 2007 and June 2010.	44
4.1	Locations of the NTS, where the releases occur (source) and of the seven stations, where the measurements are simulated (receptors).	49
4.2	Preconditions as applied for the categorisation of the hypothetical nuclear tests.	50
4.3	Overall results from the automatic analysis of 6,998 datasets including reviewed actual IMS measurements between February 2008 and February 2009 and hypothetical nuclear test contributions.	51
4.4	Assessment of the absolute contributions of the hypothetical nuclear tests at the seven stations used.	53
4.5	Number of raised flags and contributing tests under variation of the source strength.	54
4.6	Elevated Xe-133m/Xe-131m ratios at different exponential amplification factors of the source strength, given per station where they are measured.	56
4.7	Detection thresholds for the 92 releases.	57
A.1	NTS data input file used for the simulation of the hypothetical nuclear underground tests.	66

LIST OF TABLES

List of Abbreviations

ARIX	Analyzer of Xenon Radioisotopes
ARR	Automatic Radionuclide Report
ATM	Atmospheric Transport Modelling
CTBT	Comprehensive Nuclear-Test-Ban Treaty
CTBTO	Comprehensive Nuclear-Test Ban Treaty Organisation
DOE	United States Department of Energy
ECMWF	European Centre for Medium-Range Weather Forecasts
EDS	Executive Data Summary
EPOS	Executive Performance and Operational Summary
EPS	Executive Product Summary
FEB	Fused Event Bulletin
GCI	Global Communications Infrastructure
GUI	Graphical User Interface
IAEA	International Atomic Energy Agency
IDC	International Data Centre
IMS	International Monitoring System
INGE	International Noble Gas Experiment
IPF	Isotope Production Facility
MDC	Minimum Detectable Concentration
NORFY	Noble gas Review and Final analysis
NPP	Nuclear Power Plant
NTS	Nevada Test Site
OSI	On-Site Inspections
PM	Photo-Multiplier
PrepCom	Preparatory Commission

LIST OF ABBREVIATIONS

PTBT	Partial Test-Ban Treaty
PTS	Provisional Technical Secretariat
REB	Reviewed Event Bulletin
ROI	Region Of Interest
RRR	Reviewed Radionuclide Report
SAINT	Simulation Assisted Interactive Nuclide review Tool
SAUNA	Swedish Automatic Unit for Noble gas Aquisition
SEB	Standard Event Bulletin
SEL	Standard Event List
SID	Sample Identification (Number)
SOH	State Of Health
SPALAX	Système de Prélèvements et d'Analyse en Ligne. d'Air pour quantifier le Xénon
SQL	Standard Query Language
SRS	Source Receptor Sensitivity
SSEB	Standard Screened Event Bulletin
SSREB	Standard Screened Radionuclide Event Bulletin
vDEC	virtual Data Exploitation Centre
WGB	Working Group B
ZNF	Carl Friedrich von Weizsäcker-Zentrum für Naturwissenschaft und Friedensforschung (Centre for Science and Peace Research of the Hamburg University)

1 Introduction

Nuclear weapons and their testing pose a threat to international security and humankind. Since the development of nuclear weapons in 1945 more than 2000 nuclear weapons have been exploded. Since the entry-into-force of the Partial Test-Ban Treaty (PTBT) in 1962 almost all nuclear weapon tests have been conducted underground but not decreased in numbers. The Comprehensive Nuclear-Test-Ban Treaty (CTBT) which was opened for signatures in 1996 bans all nuclear tests, including those underground. Even without legally having entered into force so far, it nearly accomplished putting an end to nuclear explosions. To guarantee this success and to reach the entry-into-force and universality it is crucial to have a reliable verification regime. Therefore, a monitoring system including 80 radionuclide stations all over the world is being installed, which acquires gigabytes of data every day. Most of the collected data does obviously not indicate nuclear events and is therefore of little interest for CTBT verification. Computer algorithms are very helpful in supporting the analysts to handle all incoming data and focus on the most significant samples only. In order to classify all samples they are categorised in certain levels, that depend on the categorisation concept. Such an algorithm categorising noble gas spectra without human intervention in five levels is developed and validated in respect to false alarms in Sec. 3.

Nuclear explosives use the energy released through fission of U-235 or Pu-239. Most of these fission products are radioactive and can be identified with existing detectors, which are very sensitive. Noble gases are chemically inert and remain gaseous. They are therefore most likely to escape even from an underground nuclear explosion designed for containment and remain in the atmosphere without being washed out. The xenon isotopes Xe-131m, Xe-133m, Xe-133 and Xe-135 have the best qualified fission yields and half lives: long enough to enable reliable detection and short enough to minimise memory effects in the atmosphere. Radioxenon can be used as explicit evidence of a nuclear explosion.

A major challenge for the International Monitoring System is to distinguish between possible nuclear explosions and other sources. Civil sources as nuclear power plants (NPP) and medical isotope production facilities (IPF) release radioactivity, which can resemble the releases from nuclear explosions. Evaluating not only absolute concentrations but also their ratios can help to distinguish between civil sources and nuclear explosions, as the releases have distinct characteristics.

In order to classify recorded events, categorisation concepts were developed. The categorisation concept which is currently being implemented at the IDC uses absolute concentrations for categorisation and xenon ratios as additional flag. The algorithm proposed here enhances the categorisation concept by including xenon ratios as two additional levels resulting in a five level categorisation concept.

In Sec. 4 it is investigated whether nuclear underground tests conducted before the negotiations of the CTBT would have been detected with part of the verification system

available today and the developed algorithm. Due to time and computer performance constraints not the whole verification system is simulated, but only part of it. For similar reasons only one ground zero is assumed. At first the basic knowledge and state of research is recapitulated in Sec. 2.

2 State of research

To enforce the CTBT, a verification system has been developed that is designed to detect any nuclear explosion with an explosive yield equivalent of at least 1 kt TNT [15, 16]. This is equivalent to a release of 1 PBq Xe-133 activity, for underground tests a 10% release with a duration of 12 hours is assumed [17]. The verification system consists of the International Monitoring System (IMS), the International Data Centre (IDC), the Global Communications Infrastructure (GCI), Consultation and Clarification, On-Site Inspections (OSI) and Confidence-building measures (CBM).

The IMS collects continuously data (24 hours per day, 7 days per week), which are sent to the IDC in Vienna via the GCI. This leads to a data-stream into the IDC of more than 10 Gigabyte per day. In cases of detections, the Consultation and Clarification mechanisms will be enforced and, if necessary, OSI's. CBM's contribute to avoid misunderstandings and false alarms. For the course of this work the IMS and IDS are most relevant, which are therefore further described in the succeeding subsections 2.1 and 2.2. Very comprehensive information about all mentioned mechanisms and all other CTBTO related issues are available on the CTBTO website [1].

2.1 Data acquisition

The IMS of the CTBTO consists of 321 stations, of which 261 are already certified and working [1]. These stations are located in 89 countries, distributed all over the world as shown in Fig. 2.1. To detect all nuclear explosions, whether they are atmospheric, underwater or underground, four different kinds of signals are monitored: seismic, hydroacoustic, infrasound and radionuclides.

The first three are summarised as the so-called waveform technologies. Most of the IMS stations are seismic stations, 170 in total. 50 primary stations of these provide continuously data to the IDC as all other IMS stations, while the other 120 seismic stations are auxiliary, used for clarification purposes only. Another 11 IMS stations are located under water in the oceans, equipped with hydrophones and looking for underwater explosions. This apparently low number is well justified as the hydroacoustic waves easily propagate through the oceans, hardly absorbed or reflected by barriers. The Infrasound network consists of 60 stations, appavelled with infrasonic sensors. The waveform technologies can in general differentiate well between earthquakes and explosions, but not between chemical and nuclear explosions. The yield of the explosion can however indicate a nuclear explosion. The majority of the waveform stations are using seismic sensors, as nuclear underground explosions are much harder to detect as those taking place underwater or in the atmosphere, because the emerging radioactivity is much more likely to be contained.

The fourth technology uses radionuclides, which completes the verification system as only radionuclides can indicate whether an explosion, detected by the three waveform

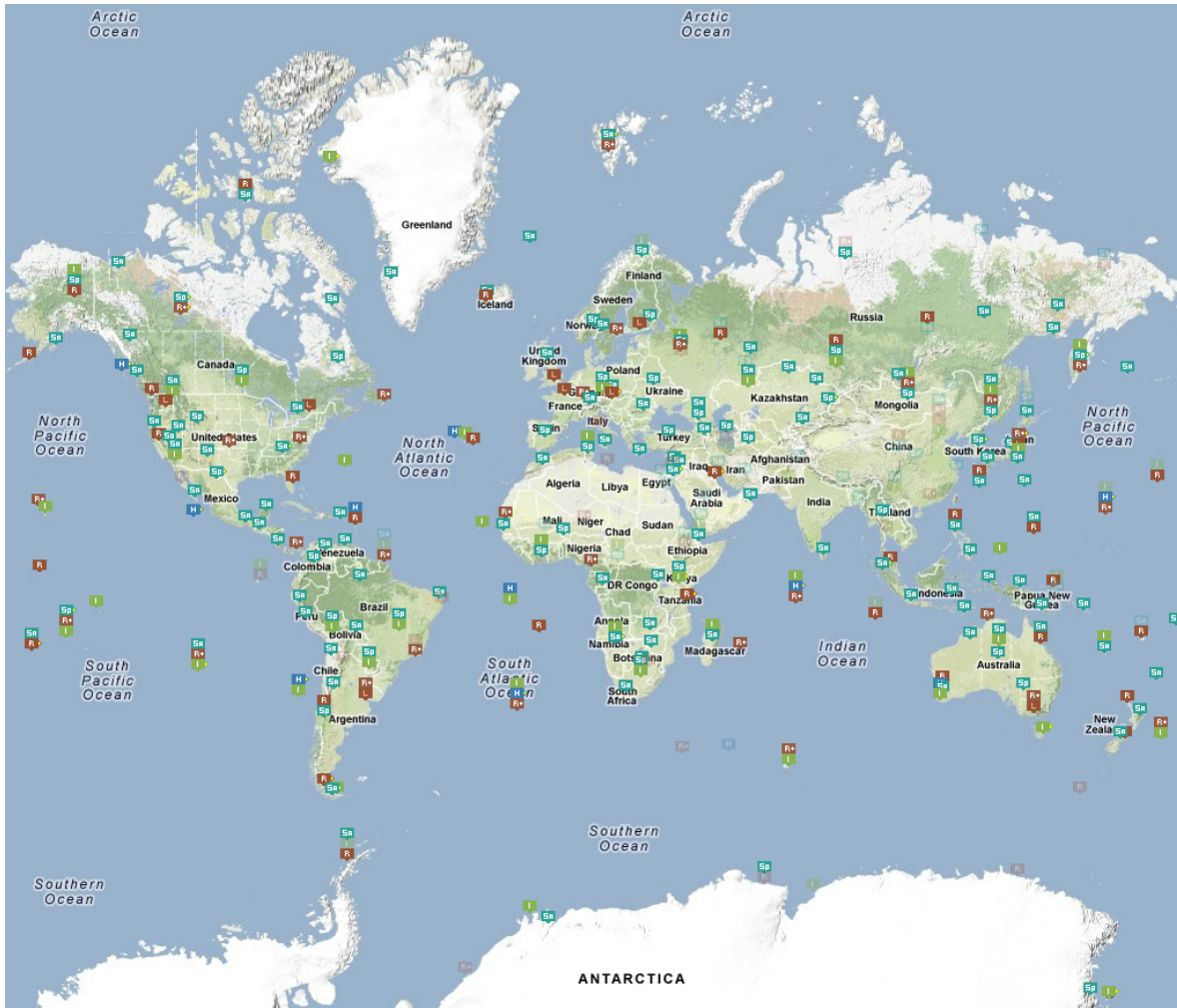


Figure 2.1: World map with all stations of the International Monitoring System of the CTBTO. [1]

Sp: primary seismic station; Sa: auxiliary seismic station; H: hydroacoustic station; I: infrasound station; R: radionuclide station; R+: radionuclide station with noble gas; L: radionuclide laboratory

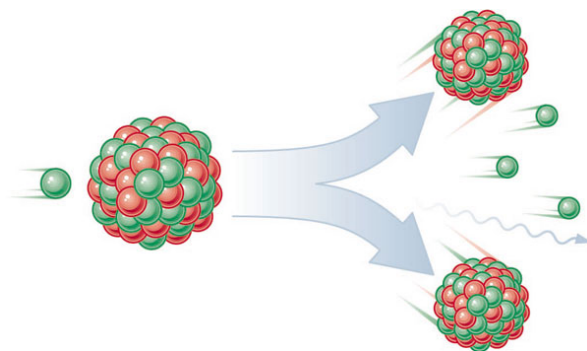


Figure 2.2: Simplified scheme of a stimulated nuclear fission. [2]
 Stimulated by a neutron (green), coming from the left a nucleus fissions into two nuclei. In addition several neutrons are released as well as more energy in form of gamma rays.

technologies, might have been a nuclear test or not. The completed IMS network will include 80 radionuclide stations looking for radioactivity in the air. All stations are capable of detecting radioactive particulates and half of them also radioactive noble gases. This will be discussed further in the next section. In addition to these stations, 16 radionuclide laboratories exist, which have own detectors and can also analyse supplementary and independently the samples taken at the radionuclide stations.

2.1.1 Radionuclide technology

A nuclear fission weapon gains its energy from fission reactions as outlined in Fig. 2.2. Induced by a neutron, a fissile core like uranium-235, plutonium-239 or others splits into two fission products, emitting further neutrons which keep the chain reaction alive by fissioning other fissile isotopes. In addition more energy in form of gamma rays is released. Thermonuclear weapons on the other hand obtain most of their energy through fusion, but also need a primary fission part, which provides the energy necessary to initiate the secondary fusion reaction. Therefore, in every nuclear explosion fission products are produced which are generally referred to as the “smoking gun” of nuclear explosions [18]. The same is true for neutron activation products which arise from neutron captures during the chain reaction. Figure 2.3 shows the decay chain from fission neutron induced fission of Pu-239. The states are colour coded according to their half-life, which is also given under the state (yellow 1–10s, red 10s–1min, pink 1–10min, blue 10min–1h and white >1000y and stable). Black indicates CTBT relevant nuclides, which all have half-lives between 6h and 1000y. In addition, the branching ratios are given. The numbers within the white squares to the right are the cumulative yields.

In 1999, De Geer identified 92 relevant nuclides, which were later agreed on as working basis of radionuclide reporting [19]. The full list as well as a very comprehensive discussion can be found in Ref. [20]. However, this list includes particles only, but

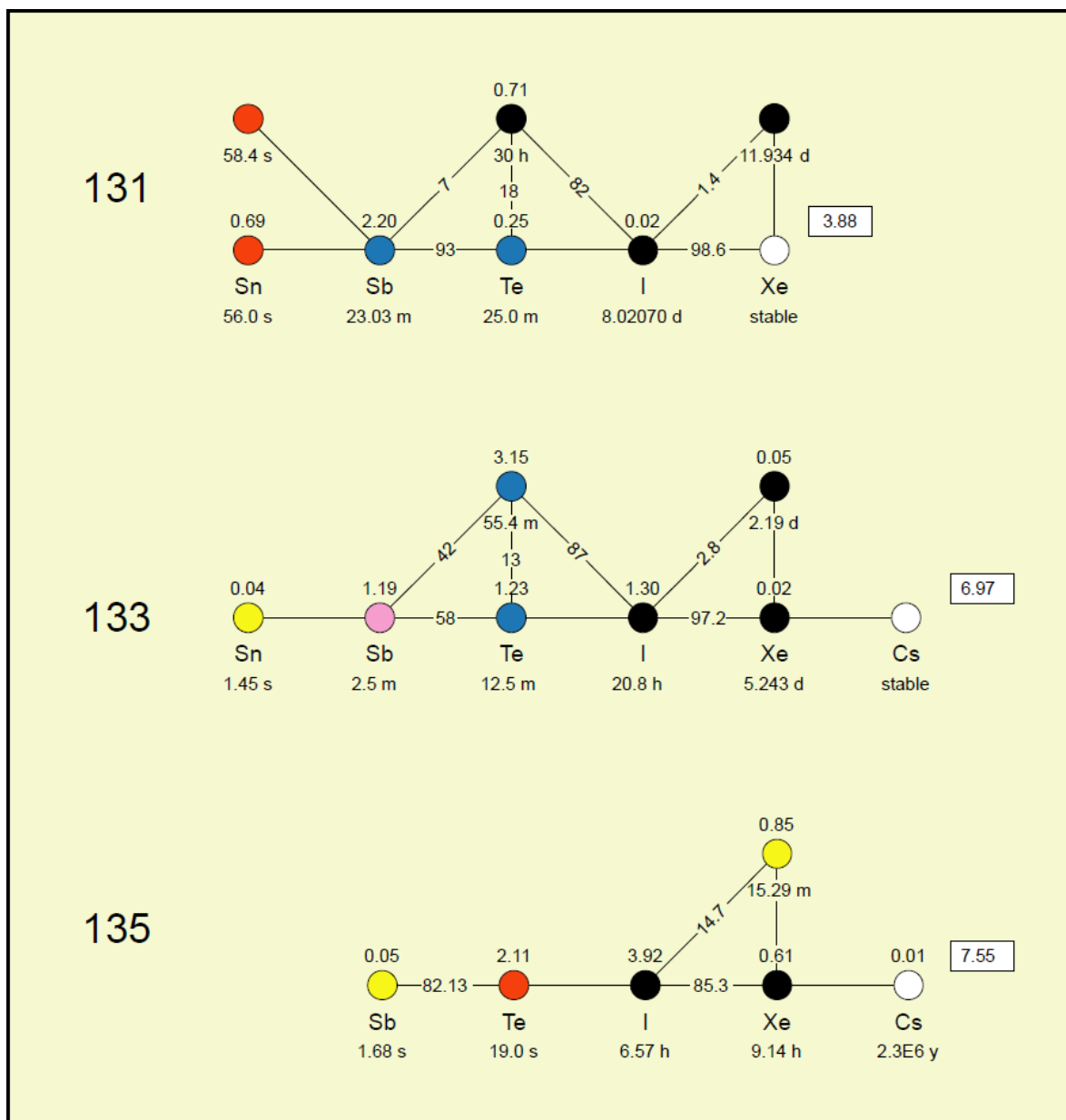


Figure 2.3: Isobaric decay chains from fission neutron induced fission of Pu-239. [3, 4] The states are colour coded according to their half-life, which is also given under the state (yellow 1–10 s, red 10 s – 1 min, pink 1 – 10 min, blue 10 min – 1 h and white >1000 y and stable). Black indicates CTBT relevant nuclides, which all have half-lives between 6h and 1000y. In addition the branching ratios are given. The numbers within the white squares to the right are the cumulative yields.

no gases, even if the latter might be as capable of indicating nuclear explosions as the former. Actually, noble gases have the potent property of being chemically inert and are therefore much more likely to enter the atmosphere while particulates are contained, for example if the nuclear explosion takes place deep underground.

At the same time, also in 1999, the International Noble Gas Experiment (INGE) was initiated to develop systems for monitoring noble gases. For CTBTO purposes, the four xenon isotopes Xe-133, Xe-135, Xe-131m and Xe-133m have proven to be the most relevant. The most important reasons are the cumulative yields from U-235 and Pu-239 (compare Fig. 2.3), the half-lives and the low natural background. Stable xenon is an atmospheric trace gas with a constant atmospheric concentration of $0.087 \frac{ccm}{m^3}$ [21]. Table 2.1 shows the half-lives of the four relevant isotopes lying between 9.14 hours and 11.84 days. These are long enough to escape from the underground and to propagate through the atmosphere and short enough to avoid overwhelming memory effects in the atmosphere.

Within the INGE, four systems were developed: The Swedish Unattended Noble gas Analyzer (SAUNA, by now SAUNA II has been introduced, both will be referred to as SAUNA in this work) in the Kingdom of Sweden, the Système de Prélèvements et d'Analyse en Ligne d'Air pour quantifier le Xénon (SPALAX) in the Federative Republic of France, the Analyzer of Xenon Radioisotopes (ARIX) in the Russian Federation and the Automated Radioxenon Sampler Analyzer (ARSA) in the United States of America. 19 of the 21 certified radionuclide stations with noble gas are SAUNA and SPALAX stations, only in Russia ARIX is used, which works similar to the SAUNA and ARSA has not been implemented at all.

All detector types collect the samples in the same way. During the collection or sampling time t_c , the ambient air is soaked in with a flow rate of at least $0.4 \frac{m^3}{h}$ [22]. Unwanted substances as for example aerosols, water, radon and oxygen are removed by filters and by heating. Xenon itself is then separated from the air by adsorption on activated charcoal. Thereafter the spectrum is measured with the according detector during the acquisition time t_a . The SPALAX system relies on high resolution gamma spectroscopy, SAUNA and ARIX on beta-gamma coincidence. The sampling and purification of xenon as well as the whole measurement process has been very well described by Paul R. J. Saey in [22].

2.1.1.1 High resolution gamma spectroscopy The Système de Prélèvements et d'Analyse en Ligne d'Air pour quantifier le Xénon uses HPGe (High Purity Germanium) detectors. From Tab. 2.1 and Fig. 2.4 it can be seen that the gamma emissions in the energy region up to 300 keV from the four relevant xenon isotopes overlap. This is especially true for the strongest peaks in the X-ray region. The most outstanding are the 81 keV peak of Xe-133, which can be detected the best, and the 249.8 keV peak of Xe-135. This is more difficult for Xe-133m at 233.2 keV and especially Xe-131m at 164 keV.

Table 2.1: Half lives, decay energies and intensities and radiation types of the four relevant radioxenon isotopes and the biggest background emitter lead. [11, 12]

Isotope	Half life	Decay energy (keV)	Decay intensity (%)	Radiation type
Xe-131m	11.90 d	30.4	54.0	X-ray (average energy)
		163.9	2.0	Gamma ray
		129.0	60.7	Conversion electron
Xe-133	5.24 d	31.6	48.9	X-ray (average energy)
		76.6	0.2	Gamma ray
		81.0	37.0	Gamma ray
		160.6	0.1	Gamma ray
		45.0	54.1	Conversion electron
Xe-133m	2.19 d	346.0	100.0	Beta (endpoint energy)
		30.4	56.3	X-ray (average energy)
		233.2	10.3	Gamma ray
Xe-135	9.10 h	199.0	63.1	Conversion electron
		31.6	5.2	X-ray (average energy)
		249.8	90.0	Gamma ray
		608.2	2.9	Gamma ray
Pb-214	0.45 h	214.0	5.7	Conversion electron
		910.0	100.0	Beta (endpoint energy)
		78.7	19.8	X-ray (average energy)
		242.0	7.3	Gamma ray
		351.9	35.6	Gamma ray
		204.7	6.8	Conversion electron
	205.5	45.9	Beta (endpoint energy)	
	225.6	40.2	Beta (endpoint energy)	

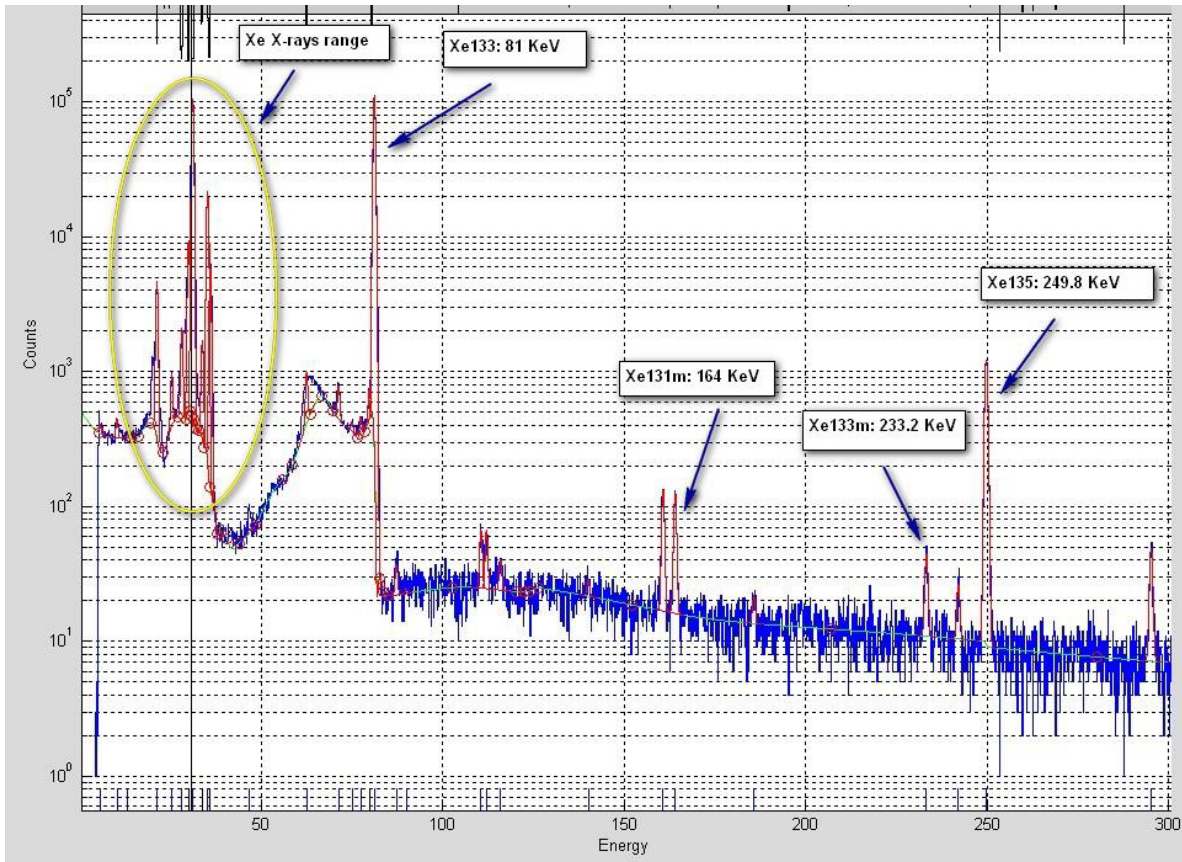


Figure 2.4: Gamma ray spectrum between 0 and 300 keV. [5]
The characteristic peaks of Xe-133 are at 81 keV, Xe-131m at 164 keV, Xe-133m at 233.2 keV and Xe-135 at 249.8 keV.

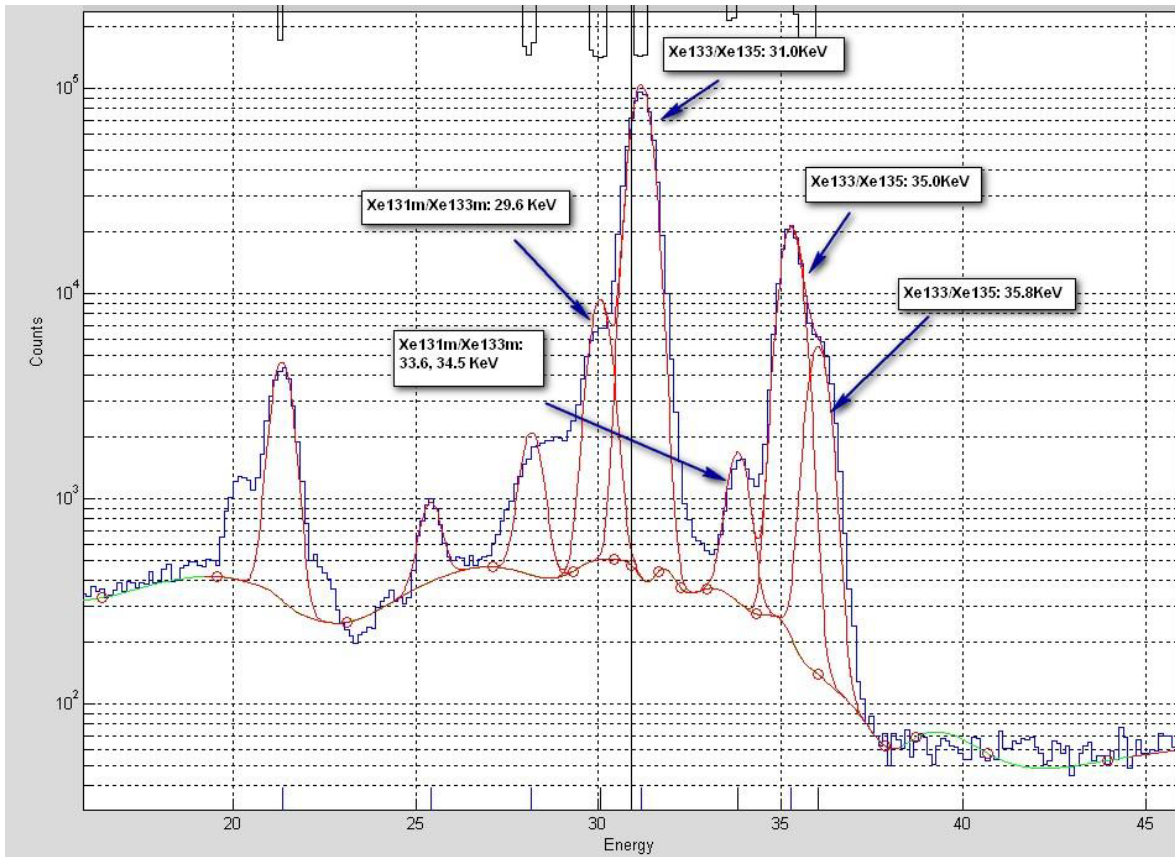


Figure 2.5: X-ray-spectrum between 15 and 45 keV. [5]

The peaks can hardly be resolved, however Xe-131m and Xe-133m can be mutually identified at 29.6 keV and 33.6 and 34.5 keV respectively, as well as Xe-133 and Xe-135 at 31.0 keV, 35.0 keV and 35.8 keV.

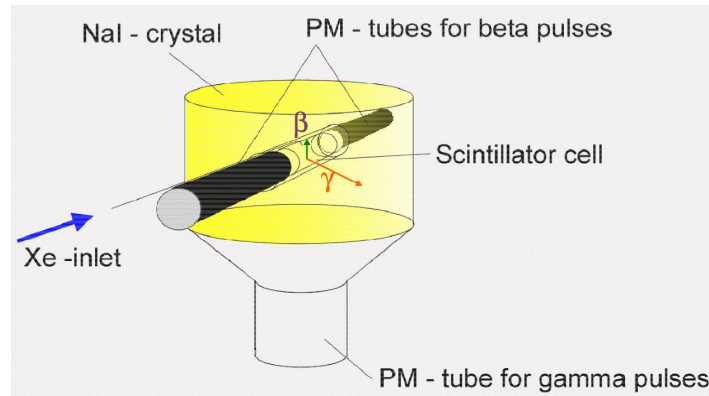


Figure 2.6: Beta-gamma detector. [5]

The sample is inserted through the Xe-inlet. Electrons from beta decay or internal conversion are detected in the two scintillator cells. The set-up is surrounded by a NaI crystal, in which the coinciding gammas trigger electric pulses which are amplified in the PM tube.

Figure 2.5 shows a close-up of the x-ray region at an energy between 15 and 45 keV. Here, the overlap is even stronger, as well as the signals itself. The figures show that a high resolution is necessary, particularly in the x-ray region in order to determine Xe-131m. These high technological requirements can be met by high purity germanium crystals, which need to be cooled by an electric cryostat and provide a high resolution at the cost of relatively low efficiency. Therefore, the intended spectrum acquisition time is set to be 24 hours. The measurement of radioxenon activity concentrations has been well described by Auer *et al.* [21] and SPALAX by Fontaine *et al.* [23].

2.1.1.2 Beta-gamma coincidence measurements SAUNA and ARIX both use NaI (sodium-iodine) crystals to detect gamma rays and scintillators to detect electrons from a beta decay or internal conversion. Every SAUNA system consists of two detectors as shown in Figure 2.6. The sample is inserted into the cylindrical scintillator cell through a stainless steel pipe (Xe-inlet). Two photomultiplier-tubes (PM-tubes) are attached at both ends of the scintillator in order to detect the beta pulses. The gamma rays are detected in the surrounding NaI-crystal which sits itself on another photomultiplier. The SAUNA system is well explained in [11] by Ringbom *et al.*

Thanks to the high efficiency of NaI-detectors, the acquisition time is only half as long as for SPALAX systems, i.e. around 12 hours. At the same time, the resolution is much lower compared to germanium crystals. The additional coincidence measurement of electrons compensates for the relatively low resolution, as they allow to still identify all four relevant xenon isotopes in a reliable way, see Sec. 2.2.1.

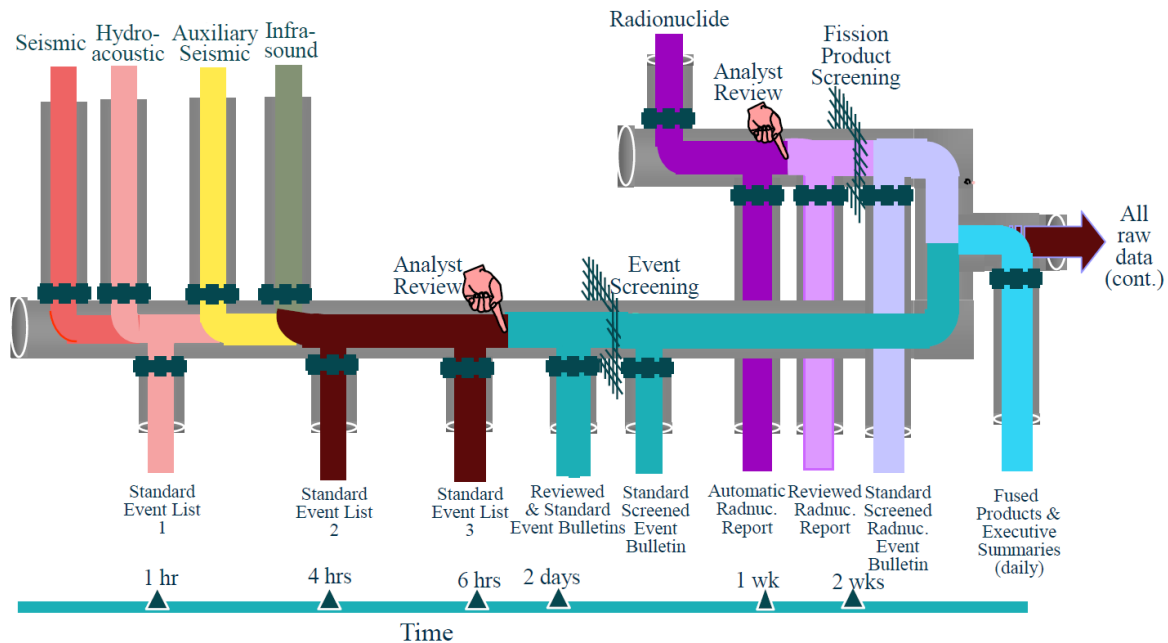


Figure 2.7: Scheme of the IDC pipeline. [6]

The evaluation process takes much longer for the radionuclides than for the waveform technologies.

2.2 Data processing at the International Data Centre

All data collected by the IMS stations are sent via the GCI to the IDC, where the analysis and interpretation takes place. All data products are prepared and issued “without prejudice to final judgements with regard to the nature of any event, which remain the responsibility of States Parties” (Protocol to the CTBT [1]). The judgement whether a detected event is a nuclear explosion or not, is never made by the CTBTO, but only by the state parties to the CTBT. It is never made by the IDC or PTS, who only provide information as comprehensive as possible to enable the State Parties to come to a profound decision.

Figure 2.7 shows the so-called IDC pipeline. The raw data from the IMS is provided by the different stations (upper part in Fig. 2.7) and runs through several processing steps. The processing level increases towards the bottom and towards the right hand side in Fig. 2.7, The occurrence of the event marks the starting time at $t = 0$ (lower left in Fig. 2.7, increases to the right). The first available data is waveform technology data, the radionuclide data (particulates and noble gases) is available only later as the sampling, decaying and acquisition takes several days. All data is analysed automatically first, from where the Standard Event List 1, 2 and 3 (SEL1, SEL2 and SEL3) for the waveforms and the Automatic Radionuclide Report (ARR) for the radionuclides emerge. SEL1 includes only primary seismic and hydroacoustic data and is available as fast as

one hour after the event. The SEL2 reports additionally include data from the auxiliary seismic and infrasound stations, as well as late arriving seismic and hydroacoustic data. SEL3 adds in turn late arriving data from the auxiliary seismic and infrasound stations. These are reviewed by trained analysts which leads to the Reviewed & Standard Event Bulletin (SEB and REB) and the Reviewed Radionuclide Report (RRR), respectively. The next step is the event screening, where all natural and man-made but non-nuclear events are screened out. For example, this can be earthquakes for the waveforms and samples without multiple anthropogenic nuclides in the case of radionuclides. From that, the much less comprehensive and much more focused Standard Screened Event Bulletin (SSEB) and Standard Screened Radionuclide Event Bulletin (SSREB) result, which are merged into the daily Fused Event Bulletin (FEB) and the Executive Data Summary (EDS), the Executive Product Summary (EPS) and the Executive Performance and Operational Summary (EPOS). The State Parties have access not only to all reports and summaries, but also to the raw data.

From Fig. 2.7 can be seen that the radionuclide analysis takes much longer than that of the waveform technologies. Improvements that can speed up the former are therefore needed. The presented algorithm shall categorise the samples of the ARR to help the analyst prioritise and improve the human-made analysis.

2.2.1 Noble gases

The automatic analysis (for the ARR) is done by the scripts `AUTO_SAINTE` for gamma spectra (from SPALAX stations) and `BG_ANALYZE` for beta-gamma coincidence spectra (SAUNA/ARIX), which have obviously no graphical user interface (GUI). `SAINTE2` and `NORFY` are used to review the automatic analysis for gamma and beta-gamma spectra respectively. `SAINTE` is the acronym of Simulation Assisted Interactive Nuclide review Tool; `NORFY` of Noble gas Review and Final analysis.

Figure 2.8 shows the GUI of `SAINTE2`. All relevant isotopes can be analysed in detail. The regions of interest of the energy spectrum are in the case of Xe-135 (in Fig. 2.8 selected in the green area) the energies around 31.6 keV, 249.8 keV and 608.2 keV. `SAINTE2` calculates the corresponding concentrations from the (corrected) peak areas and provides additional information like the error and detectability, for the latter see Sec. 2.2.3.

Figure 2.9 shows the GUI of `NORFY`, the blue bars have been inserted to protect sensitive information like the sample ID (SID), station code, and collection and acquisition start and stop. Here, the analyst can directly see whether the state of health (SOH) criteria like collection and acquisition time, xenon volume, *MDC*, reporting and processing time, gas background and radon count are fulfilled or not (green mark), see Sec. 2.2.2 for more information on the SOH information. The display can be switched from the sample itself to the gas background or the quality control spectrum via the In the “Tools” section. All spectra show the gamma energy as a function of the beta energy. In

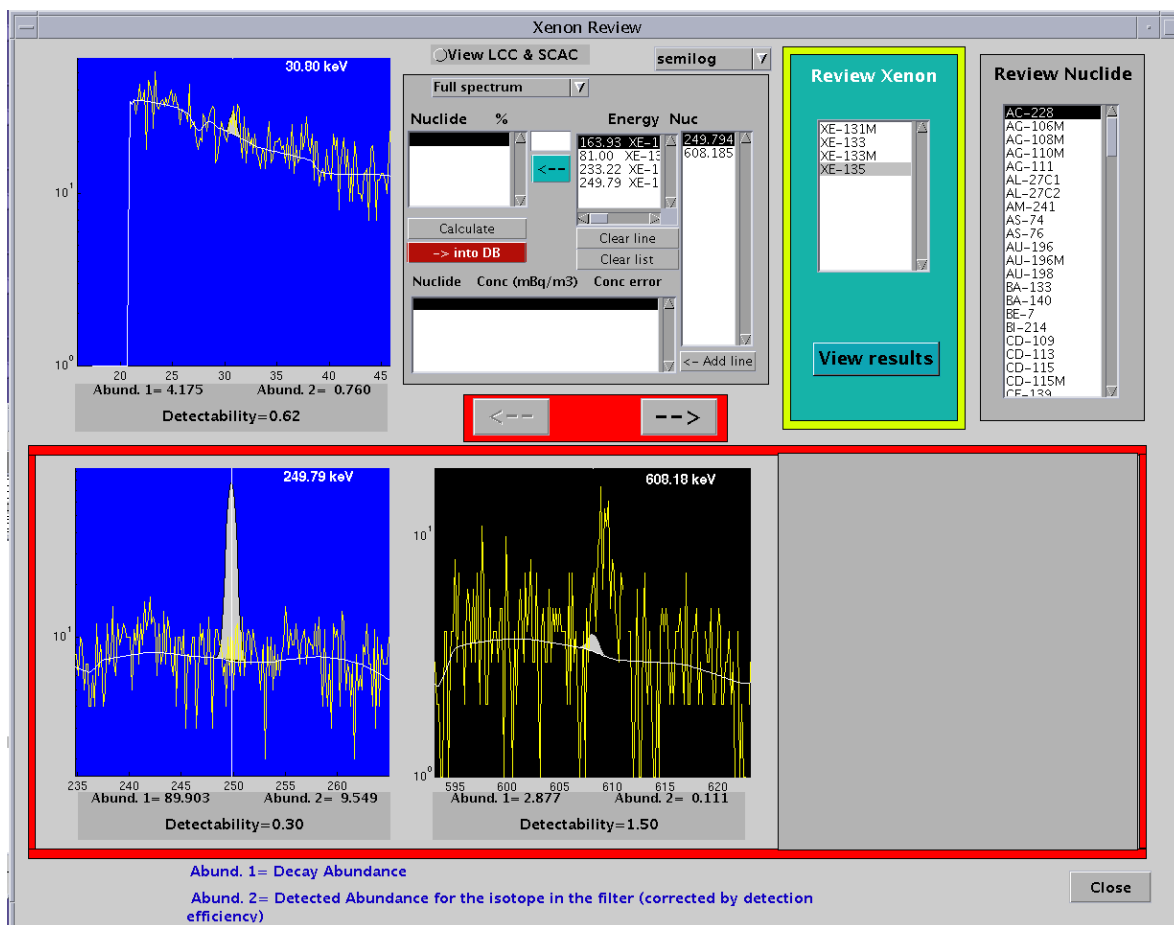


Figure 2.8: GUI of the high resolution gamma spectra analysis software SAINT2. [5] High resolution gamma ray spectra are reviewed mainly by adjusting the calibration and identifying the single peaks of the four relevant radioxenon isotopes (below) which can be chosen individually from the green panel and other nuclides.

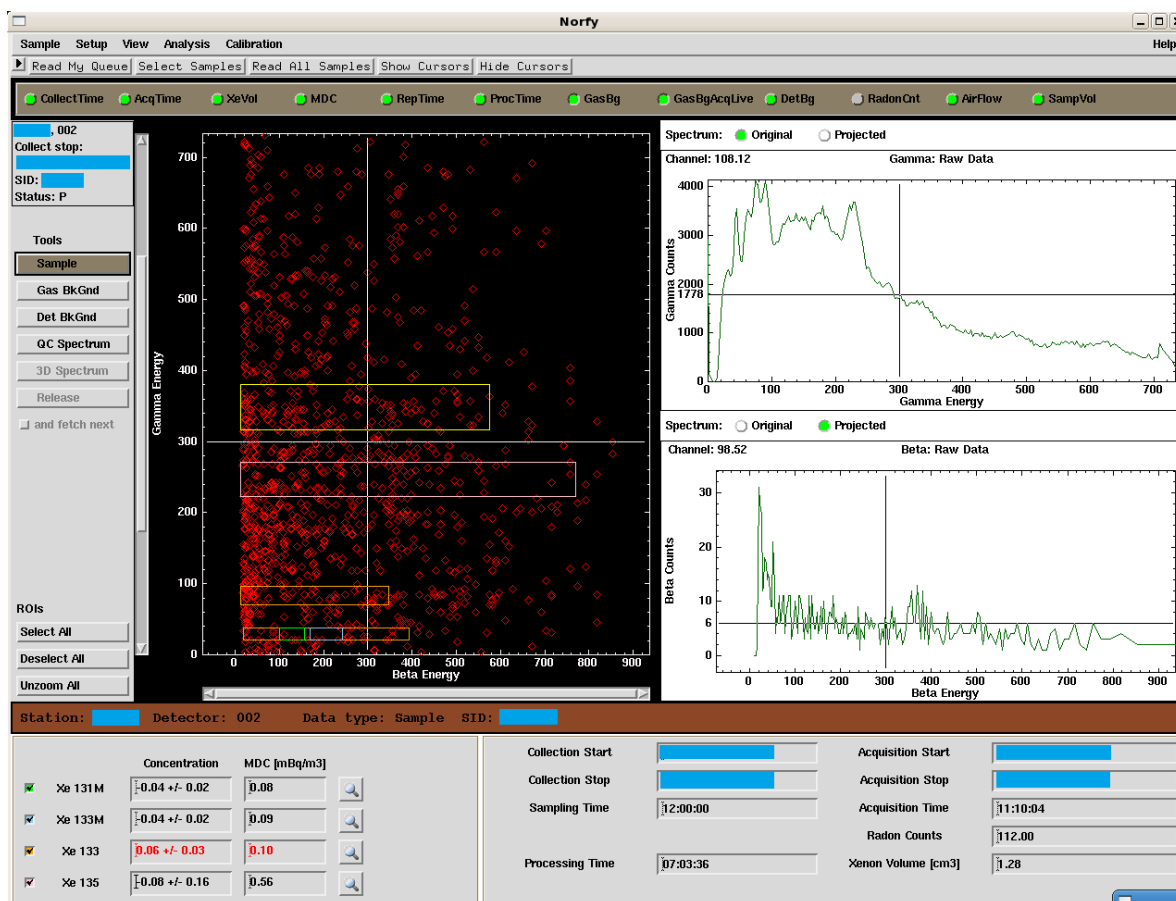


Figure 2.9: GUI of the beta-gamma coincidence spectra analysis software NORFY. In addition to the coincidence spectrum and the normal beta and gamma ray spectra, general sample and state of health information are provided. The blue bars have been added to protect sensitive information.

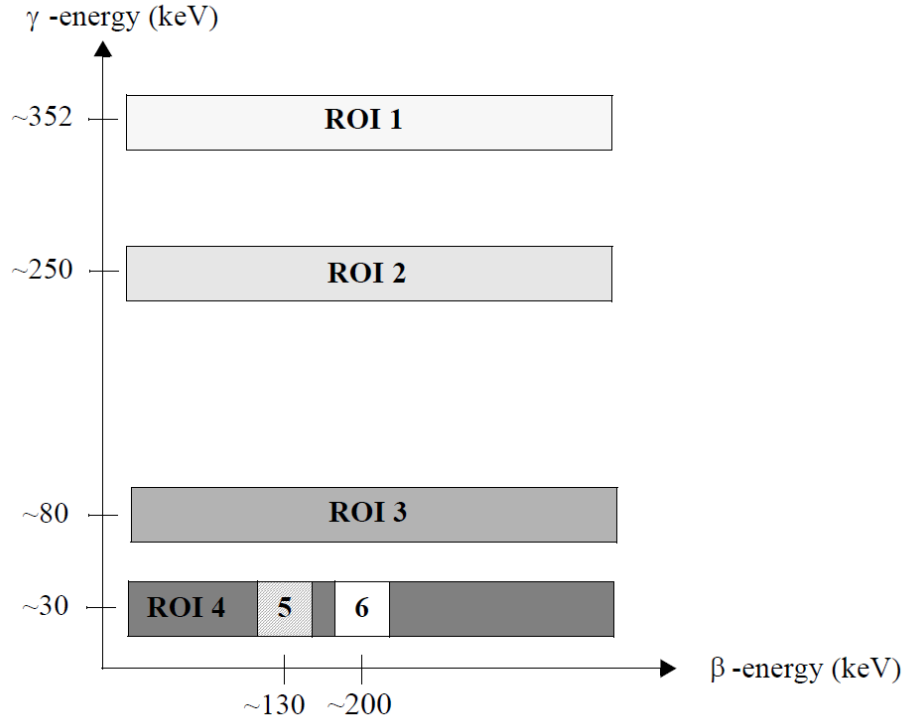


Figure 2.10: Regions of interest used to analyse beta-gamma coincidence spectra. [7] The regions of interest are used to successively determine all relevant activity concentrations, ROI 1 for Pb-214, ROI 2 for Xe-135, ROI 3 for Xe-133, ROI 4 for the metastables, including ROI 5 for Xe-131m and ROI 6 for Xe-133m. Since 2004, a scheme including 11 ROI's is implemented [24]. The additional ROI's facilitate the distinction between the two metastable isotopes.

this plot, the regions of interest (ROI) can be highlighted, which are used to determine the xenon concentrations as explained in Fig. 2.10. NORFY also provides the simple gamma and beta spectra on the right and the determined xenon concentrations as well as all relevant sample information at the bottom.

Figure 2.10 shows a scheme of a beta-gamma spectrum and the ROI's for the identification of the relevant xenon isotopes. Most of the background can already be reduced through the coincidence measurement and correction of memory effects in the detector. The remaining background in these spectra is mainly due to the decay of Pb-214. The signal in the ROI 1 at around 352 keV comes from Pb-214. Therefore, ROI 1 is used to determine its activity. The contributions according to the other ROI's are then subtracted from the latter. Xe-135 has a strong gamma line at 249.8 keV from its decay to Cs-135, which defines ROI 2 at around 250 keV. Having quantified Xe-135, its contribution to the following ROI's can again be determined and corrected. The same is true for Xe-133, whose decay to Cs-133 can be identified within ROI 3 around 80 keV.

Table 2.2: State of health categorisation for samples taken at SPALAX stations. [13]

Sampling Time	12 h	21.6	26.4	48 h
AcquisitionTime	12 h	21.6	26.4	48 h
Xenon Volume	0.87ml			
MDC	0.001 mBq/m ³	1	5 mBq/m ³	
Reporting Time	10 h	48	96 h	

The first column (white) specifies the state of health information, the following columns show the categorisation (green, yellow, red). In addition, the thresholds defining the levels are given.

Table 2.3: State of health categorisation for samples taken at SAUNA stations. [14]

Collection Time	6 h	10.8	13.2	24 h
AcquisitionTime	6 h	10.8	13.2	24 h
Xenon Volume	0.2ml	0.87ml		
MDC	0.001 mBq/m ³	1	5 mBq/m ³	
Reporting Time	10 h	48	96 h	

The first column (white) specifies the state of health information, the following columns show the categorisation (green, yellow, red). In addition, the thresholds defining the levels are given.

Both relevant metastable xenon isotopes have their strongest signal from their decay into the stable isotopes according to ROI 4, which is the X-ray region around 30 keV. To distinguish between both, now the electrons become an important factor. Xe-131m emits conversion electrons at 129 keV, while those from Xe-133m have an energy of 199 keV. This defines ROI 5 and ROI 6. A scheme including 11 ROI's is implemented since 2004, the additional ROI's facilitate the decision making in the 30 keV region [24].

2.2.2 State of health criteria

The SOH-criteria are used to assess the reliability of the measured spectra. Therefore, a number of qualities are given and classified. The most important SOH-criteria are given in Fig. 2.2 and Fig. 2.3 for both detector systems and differ only in numbers, but not in the five SOH-criteria Collection/Sampling Time, Acquisition Time, Xenon

Volume, *MDC* for Xe-133 and Reporting Time. The difference in the thresholds comes again from the different detector types as explained in Sec. 2.1.1.

In analogy to a traffic light, every single spectrum is classified either as GREEN if it has a good SOH performance, YELLOW for medium performance and RED if it is not meeting the minimum SOH-criteria.

2.2.3 Detectability

The *MDC* is defined as

$$MDC = \frac{L_D}{\epsilon \cdot I \cdot V \cdot \lambda^{-2} \cdot (1 - e^{-\lambda t_c}) \cdot e^{-\lambda t_d} \cdot (1 - e^{-\lambda t_a})}, \quad (1)$$

where ϵ is the detection efficiency, I the intensity, V the sample volume, λ the decay constant, t_c the collection time, t_d the decay time, t_a the acquisition time and L_D the detection limit, defined as

dem

$$L_D = k^2 + 2 \cdot L_C, \quad (2)$$

where k is the confidence factor, pursuant to the demanded confidence level of 95% set to $k = 1.645$ [7] and L_C the critical level defined as

$$L_C = k \cdot \sqrt{B + \sigma_B^2}, \quad (3)$$

where B is the baseline counts and σ_B the according uncertainty. The concepts of the detection limit and the critical level are well described in [25], the *MDC* in [7] and [26].

2.2.4 Potential of radioxenon ratios

Radioactive measurements are particularly interesting for CTBT verification because they have a very low natural background. However, there exist quite a number of legitimate sources from which the biggest are IPF's and NPP's. All of these emit more or less continuously radioactivity, which can resemble those coming from nuclear explosions. This issues a great challenge to the IMS which should on the one hand not raise false alarms for signals from civil sources (false positive/type I error). On the other hand, a nuclear explosion must not be considered as civil event or neglected because it coincides with a strong civil event (false negative/type II error). This is partly given by the relative high density of IMS stations which should be able to detect every event at multiple stations. The thereby increased resolution facilitates

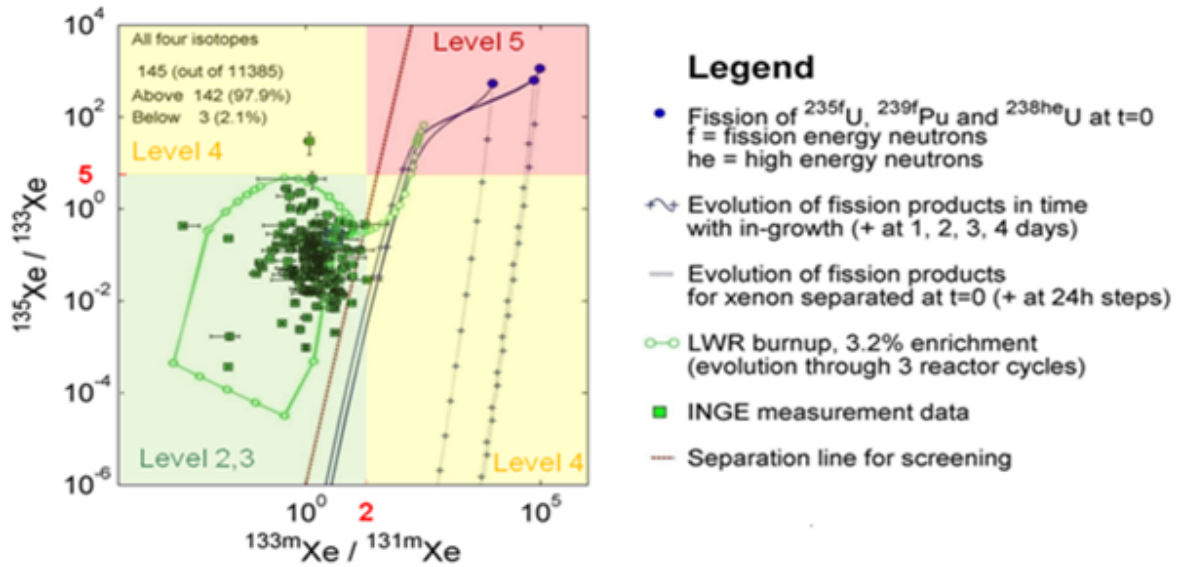


Figure 2.11: Xenon ratio $\text{Xe-135}/\text{Xe-133}$ as a function of the ratio $\text{Xe-133m}/\text{Xe-131m}$. [8]

This plot by Kalinowski *et al.* shows the potential of xenon ratios for event categorisation. The four levels and threshold proposals were added by the author.

the distinction between releases at different geographical coordinates. It is however desirable and important to still enhance the detection confidence. The definition of validated criteria to use isotopic ratios and other characteristics of measurement data to distinguish civil sources from nuclear explosions has been recognised as a key issue *inter alia* by Zähringer *et al.* [27].

Martin Kalinowski *et al.* found a way to clearly distinguish nuclear explosions from civil sources, nearly independent of source strength in absolute xenon activity concentrations but relying on their characteristic radioxenon ratios [8]. The fifteen possible combinations of the four relevant radioxenon isotopes have been evaluated and the so-called four isotopes plot presented in Fig. 2.11 might be seen as the most robust one, as it uses all four isotopes. It provides the base of the categorisation algorithm presented here. The green data points show the distribution of civil sources, taken during the INGE exercise. *Inter alia* a full nuclear light water reactor cycle can be tracked. Furthermore the simulation curves for nuclear explosions are given, as well as a separation line for screening (red). For this study, the thresholds have been set to simple numbers as indicated through the colouration and described in Sec. 3.5.

2.3 Radioxenon background

As mentioned in Sec. 2.1.1, stable radioxenon is at a constant atmospheric concentration of $0.087 \frac{ccm}{m^3}$ [21]. The releases by the biggest civil xenon emitters, i.e. NPP's and IPF's, are however an important factor for CTBT verification and have been analysed in numerous studies, e.g. in [28, 29, 30, 31, 32]. This is important to understand the origins of signals as well as to be able to distinguish between legitimate civil sources and nuclear explosions as banned by the CTBT (see Sec. 2.2.4). In this work the background is always considered, since real IMS measurements are used. This is true for the validation in Sec. 3 as well as for the hypothetic detection of nuclear tests described in Sec. 4.

2.4 Availability of radioxenon measurement data

A lot of radioxenon measurement data has been published or is generally available to the public. But when it comes to nuclear tests, security concerns prevent a lot of publications and exchange. Schoengold *et al.* from the United States Department of Energy (DOE) however published a very comprehensive report of radioactivity measurements in 1996 [33]. For other countries like for example the Russian Federation/former Soviet Union much less information is available [9], especially on radioxenon measurements. Existing studies therefore focus on those tests reported by Schoengold *et al.*, which were all conducted at the NTS in the United States of America [9, 34, 35].

Figure 2.12 shows 292 absolute Xe-133 activity releases for nuclear underground tests conducted at the NTS as a function of time, as well as the duration of the releases (horizontal bars). The notation is double logarithmic. Nearly all releases are operational (x) and only three uncontrolled (circle). Most of the operational releases are filtered with a high efficiency by a particulate air filter and charcoal filter combination (solid circle). The maximum release expected from a 1 kt TNT equivalent nuclear explosion (10^3 TBq) and the 10% release scenario (10^2 TBq) are given as dashed lines. All three uncontrolled releases exceed 10^2 TBq activity for the isotope Xe-133, but only 22 of the operational releases.

The situation is also complicated for the data acquired by the IMS of the CTBTO, although for other reasons. This data belongs to the States Party to the treaty and is therefore not publicly available. The states can however decide to share their data and so can the PTS itself if it meets formal requirements. The CTBTO is interested in sharing its knowledge and further develop its technologies, for example in cooperation with universities and also by supplying its very fast GCI to contribute to tsunami warning to give another example. However, the administrative barriers remain rather high. In order to be able to work with IMS data outside the PTS, a contract between

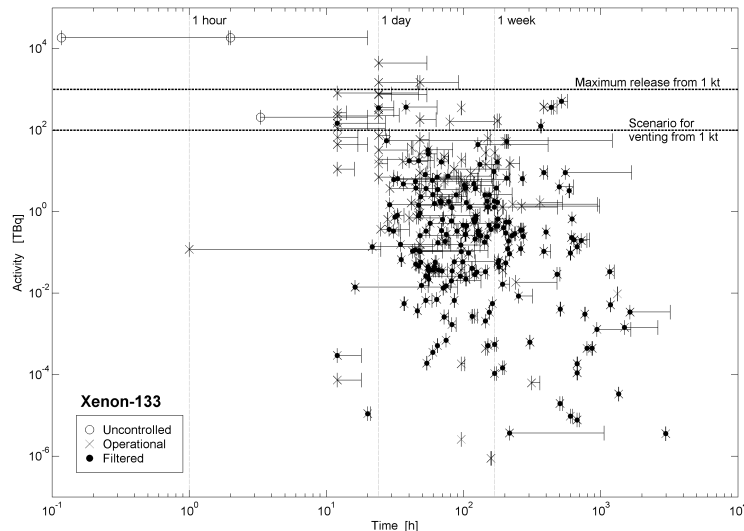


Figure 2.12: Absolute Xe-133 activities for releases at the NTS as a function of time. [9]

The activities are differentiated according to whether they belong to uncontrolled (circle), operational (x), and filtered (solid circle) releases.

the CTBTO Preparatory Commission (PrepCom) and the Hamburg University had to be concluded. Thus, IMS data could be accessed via the virtual Data Exploitation Centre (vDEC).

The CTBTO requirements include a data availability of more than 95%, with down times lower than seven consecutive days and less than fifteen days per year [23]. An assessment of the radioxenon time series has recently been made by Plastino *et al.* [36].

Stocki *et al.* did a study on the classification of radioxenon events, investigating the potential of machine learning [35]. IMS measurements were used to provide a background which was added to synthetic nuclear explosion data, based on measurements at the NTS. Instead of using ATM to simulate their propagation, statistical concepts were used to deduce realistic local radioxenon activity concentrations.

2.5 Atmospheric transport modelling

From the origin of the release the (radioactive) fission products are transported through the atmosphere, eventually passing IMS stations where they are detected. Knowing the time of arrival at a station atmospheric transport modelling (ATM) can be used to determine the release origin independently from and therefore complementary to the waveform technologies. Calculations from the arrival point (receptor) are called backwards modelling, contrary to forward models, which simulate the propagation from

known sources. In each case the source-receptor sensitivity (SRS) from one or several grid points to the rest of the grid is given, i.e. the interconnection between two grid points at specified times. The SRS can be mathematically expressed as matrix M_{ijn} [m^{-3}], where i and j indicate a discrete location and n a time interval. For backwards ATM, M_{ijn} correlates the concentration C ($Bq\ m^{-3}$) at a specified arrival point with a spatio-temporal source field S_{ijn} [Bq] [37]:

$$C = M_{ijn} \cdot S_{ijn} \quad (4)$$

The actual propagation path highly depends on the local meteorological conditions. If the resolution of the used simulation is not high enough, this can lead to altered signals [36]. In this work, the Lagrangian particle dispersion model FLEXPART 8.2 is used for all ATM simulations. The “particles” do not necessarily represent real particles but rather air parcels and can hence be used to simulate the propagation of noble gases as well as those of particulates. Relying on Lagrangian models, the parcel resolution can have a infinitesimal small resolution, there is no numerical diffusion. FLEXPART uses the simple “zero acceleration” scheme [38]:

$$X(t + \Delta t) = X(t) + v(X, t) \cdot \Delta t, \quad (5)$$

to integrate the trajectory equation [39]:

$$\frac{dX}{dt} = v[X(t)], \quad (6)$$

where X is the position vector, t the time and v the wind vector. The latter is itself composed of the grid scale wind \bar{v} , the turbulent wind fluctuations v_t and the mesoscale wind fluctuations v_m [38]:

$$v = \bar{v} + v_t + v_m. \quad (7)$$

During the propagation, the concentration of the fission product is diluted not only over space and time but intensified through radioactive decay. This is already accounted for in FLEXPART 8.2, the concentrations are reduced according to the law of exponential decay:

$$C(t + \Delta t) = c(t) \cdot e^{-\lambda \cdot \Delta t}, \quad (8)$$

where C is again the concentration, t the time and λ the decay constant, characteristic for every isotope and linked via $\lambda = \frac{\ln 2}{T_{1/2}}$ to the half-life, which is given for the four relevant radioxenon isotopes in Tab. 2.1.

3 Algorithm validation

In a first step, existing spectrum categorisation concepts are adapted and an algorithm for the automation of the categorisation is developed. The algorithm is validated with the IMS measurement data in a second step.

The Working Group B (WGB), which is the policy making organ to the CTBTO Prep-Com, gave preference to a three level categorisation concept in 2001 and again in 2011, which is currently being implemented at the IDC. The idea of a five level categorisation concept including xenon ratios was rejected due to its complexity. However, the xenon ratios are included in the 2011 endorsed three level concept as flags. Having five levels would make the categorisation concept easily comparable to the five level categorisation concept of the particulates. In this work, a categorisation concept developed by Matthias Zähringer [40] has been adapted. As proposed, a non-conclusive number of flags is introduced, which leads to up- and down-grading of the analysed samples. The first three levels of the presented categorisation concept are identical to the three level categorisation concept approved by the WGB.

The presented algorithm categorises the noble gas spectra collected by the IMS in five levels. If no xenon is detected, the sample is categorised as Level 1, if a xenon activity concentration that is typical for the specific station is measured, the sample is categorised as Level 2 and with anomalous high xenon concentrations as Level 3. If one of the two xenon ratios used for categorisation exceeds the defined threshold, the sample is categorised as Level 4, if even both ratios are exceeded, as Level 5, as already shown in Fig. 2.11.

During the analysis described in this section, a number of parameters has been introduced, which are summarised in Tab. 3.6. In order to be able to interpret the huge amount of data under variation of various parameters, the software XE has been written in cooperation with Marco Verpelli in the course of this work. The software is written in Java code and uses Standard Query Language (SQL) to retrieve the necessary information from the IDC database. Figure 3.1 shows the GUI of the XE software, the red bars have been added to protect sensitive information like the sample and station ID. In the upper left corner all sample specific informations are given, including data provided by the database, SOH informations, the calculated ratios and the categorisation. On the right hand side, station specific data on the xenon statistics is provided, below a flag summary is given (which is again station, not sample, specific). Via the panel on the bottom of the upper window the analyst can choose which data are shown in the second window, a graph of the xenon concentrations over time of the respective station is given.

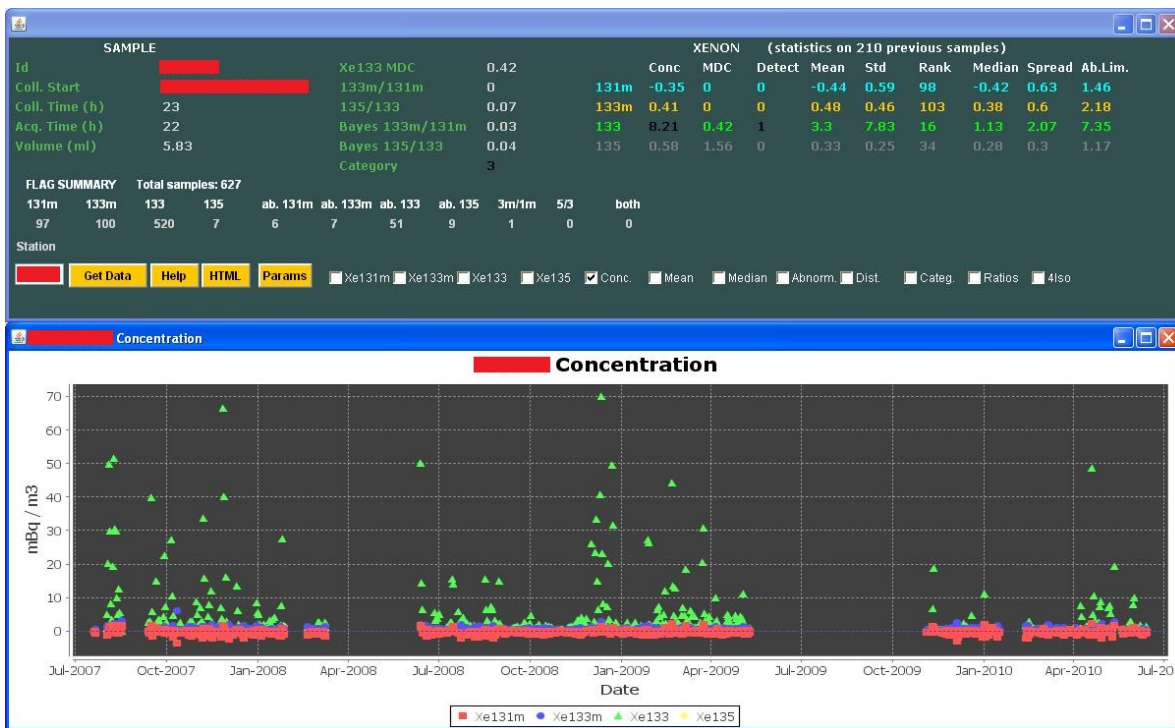


Figure 3.1: GUI of the XE software.

The XE software has been written to evaluate the huge amount of data under variation of numerous parameters, particularly regarding xenon ratios.

Table 3.1: Mutual preconditions for the categorisation of spectra from all three station types as applied for the used algorithm.

criteria	SPALAX, SAUNA II, ARIX I
gss.status	“R”, “Q” or “P”
gsd.spectral_qualifier	“FULL”
method_id	11

Table 3.2: Preconditions for the categorisation of spectra from SPALAX stations as applied for the used algorithm.

Collection Time		12 h	48 h	
Acquisition Time		12 h	48 h	
Reporting Time		10 h		96 h
Xenon Volume		0.87 ml		
MDC Xe-133		0.001 mBq/m ³	5 mBq/m ³	
MDC Xe-135		0.001 mBq/m ³		10 mBq/m ³

The first column (white) specifies the preconditions, the following columns give the according lower and upper limit (yellow). Values exceeding those limits (red) disqualify a sample for the automatic categorisation.

Table 3.3: Preconditions for the categorisation of spectra from SAUNA II and ARIX stations as applied for the used algorithm.

Collection Time		6 h	24 h	
Acquisition Time		6 h	24 h	
Reporting Time		10 h		96 h
Xenon Volume		0.2 ml		
MDC Xe-133		0.001 mBq/m ³	5 mBq/m ³	
MDC Xe-135		0.001 mBq/m ³		10 mBq/m ³

The first column (white) specifies the preconditions, the following columns give the according lower and upper limit (yellow). Values exceeding those limits (red) disqualify a sample for the automatic categorisation.

3.1 Preconditions for categorisation

A fully automatic algorithm can not simply categorise all samples. Unreviewed spectra can contain senseless, contradictory or simply wrong information, which make it difficult for an automatic algorithm to categorise them. These difficulties increase exponentially if the sample interpretations are interconnected. Therefore, preconditions have to be defined to include only such samples which are robust enough for the algorithm to work with. Only samples fulfilling the conditions defined in the Tables 3.1, 3.2 and 3.3 are considered for the analysis. The preconditions defined in Tab. 3.1 ensure that only spectra which are already processed with the standard IDC means are taken into account. Tables 3.2 and 3.3 are basing on the YELLOW SOH criteria discussed in Sec. 2.2.2. An additional criterion is introduced, the *MDC* for Xe-135. This proofs to screen out an important number of spectra which the algorithm otherwise would have difficulties to deal with.

3.2 Rank order

Every sample is given a rank number comparing it to a set of all samples taken in the previous λ_1 days at this station. As measure the absolute concentrations are used, Xe-131m for Flag 1, Xe-133m for Flag 2, Xe-133 for Flag 3 and Xe-135 for Flag 4, see Tab 3.5.

The sample with the highest radioxenon activity concentration is ranked as number one, the second highest as number two and so forth. λ_1 could for example be set to 365 days to include the samples of a whole year. Other options could be the use of samples of only the past 90 days or of the samples of the past 45 days plus those of the very last year but 45 days 'preceding'. By this last option, seasonal fluctuations would be taken into account. However, the number of samples has to be sufficiently high to guarantee reliable statistics, with down times of the stations taken into account. By choosing the set of samples this way, station characteristics like the individual background are automatically incorporated. The Rank order is not used for categorisation but for flagging only.

3.3 Identification

As already mentioned above, the identification, i. e. the decision process whether a measured concentration is above the *MDC* or not, is already implemented within today's IDC analysis. The according NID_Flag is therefore taken from the IDC database¹. According to the IDC standards, the code given in Tab. 3.4 is used. Flag 5 refers to the identification of Xe-131m, Flag 6 to that of Xe-133m, Flag 7 to that of Xe-133 and Flag 8 to that of Xe-135, see Tab 3.5.

¹gards_bg_isotope_concs.NID_Flag for SAUNA stations and rmsman.gards_xe_results.NID_Flag for SPALAX stations

Table 3.4: Identification code as implemented within the IDC

code	SPALAX	SAUNA
0	not identified	not identified
1	identified	identified
2	signal in X-ray but not in γ -region	-

3.4 Abnormal concentration

The abnormal concentration is defined to highlight such samples, where (at least) one xenon concentration is essentially higher than one does expect from the individual station history. It is based on the set of previous samples defined in Sec. 3.2. The threshold is defined as:

$$\begin{aligned} C_{tr} &= P(50) + \lambda_2 \cdot [P(75) - P(25)] \\ &= \text{Median} + \lambda_2 \cdot \text{Spread} , \end{aligned} \tag{9}$$

where $P(x)$ is the percentile and λ_2 the abnormal concentration factor. If Xe-131m is at abnormal concentration Flag 9 is raised, for an abnormal Xe-133m concentration Flag 10, for Xe-133 Flag 11 and for Xe-135 Flag 12, see Tab 3.5.

3.5 Isotopic ratios

A simple calculation of the ratios from the xenon activity concentrations acquired by the IMS stations maintains all statistical fluctuations. This leads to a very broad distribution of ratios which does not at all resemble what one would expect from Fig. 2.11. To reduce false alarms (false positives), the simple ratio is calculated and shown in the GUI of the XE software, but not used for categorisation. Instead, the Bayesian confidence limits are used, which allow a more reliable categorisation. The calculation of the Bayesian limits has been well described by Matthias Zähringer in [40] and the underlying method in [41].

The upper and lower Bayesian confidence limits C_i^+ and C_i^- are defined as

$$C_i^+ = C_i + S_i \cdot f^{-1} \left[1 - \lambda_3 \cdot f \left(\frac{C_i}{S_i} \right) \right] , \tag{10}$$

$$C_i^- = C_i - S_i \cdot f^{-1} \left[1 - \lambda_4 \cdot f \left(\frac{C_i}{S_i} \right) \right] , \tag{11}$$

where C_i is the measured xenon activity concentration, S_i the according error and $i = Xe - 131m, Xe - 133m, Xe - 133, Xe - 135$ indicates the relevant xenon isotopes.

λ_3 and λ_4 are two parameters used to fine-tune the categorisation algorithm and $f(x)$ is the cumulative Gaussian distribution function:

$$f(x) = \frac{1}{\sqrt{2\pi}} \int_{-\infty}^x e^{-\frac{z^2}{2}} dz . \quad (12)$$

λ_3 is selected to be smaller than λ_4 , with the result that C_i^+ is bigger than C_i^- . Therefore, the xenon ratios

$$\frac{C_{\text{Xe-133m}}^-}{C_{\text{Xe-131m}}^+} > T_1 \text{ (Flag13)}, \quad (13)$$

$$\frac{C_{\text{Xe-135}}^-}{C_{\text{Xe-133}}^+} > T_2 \text{ (Flag14)}, \quad (14)$$

which are used for the categorisation are conservative estimates, as well as the third ratio

$$\frac{C_{\text{Xe-133m}}^-}{C_{\text{Xe-133}}^+} > T_3 \text{ (Flag15)}, \quad (15)$$

which is reported but not used for categorisation.

Often, not all four relevant radioxenon isotopes are detected, but only some of them. However, no detection does only mean that the activity concentration could not be determined as it was below the *MDC*. The radioxenon ratios are therefore not only calculated in cases in which the two according isotopes are detected but also if only one could be accounted for. The other isotope concentration is then substituted through the *MDC* as the highest possible activity concentration below the detection threshold (any higher concentration would have been detected). This method leads to conservative assumptions, but one has to bear in mind that when dealing with ratios, these can still be shifted in both directions. The use of the *MDC* as substitute for non-identified isotopes has already been proposed by Kalinowski *et al.* [8]. The combination of the two different statistical concepts of the *MDC* on the one and the Bayesian on the other hand might introduce some inconsistency. It is however justified through the high number of samples which can be additionally included in the automatic analysis compared to previous concepts. Otherwise, no information could be provided at all. The *MDC* is only used in those cases, where an analysis would otherwise not be possible at all since the concentrations are unknown.

3.6 Source-receptor sensitivity fields and state of health information

The origin of a signal is a very important property in order to assess an event. In the case of the waveform technologies, the origin can in general be determined from the

Table 3.5: Categorisation Levels as used by the algorithm.

	Flag	min. Level
1	Xe-131m	-
2	Xe-133m	-
3	Xe-133	-
4	Xe-135	-
rank order		
5	Xe-131m	2
6	Xe-133m	2
7	Xe-133	2
8	Xe-135	2
detected		
9	Xe-131m	2
10	Xe-133m	3
11	Xe-133	3
12	Xe-135	3
at abnormal concentration		
13	$\frac{C_{Xe-133m}^-}{C_{Xe-131m}^+} > T_1$	4
14	$\frac{C_{Xe-135}^-}{C_{Xe-133}^+} > T_2$	4
15	$\frac{C_{Xe-133m}^-}{C_{Xe-133}^+} > T_3$	-
16	SRS fields	-
17	SOH	-

signal itself. Radioactivity on the other hand does not directly inherit this information, but it has to be extracted from other information. Atmospheric field information can help to determine the origin of radioactive plumes, as discussed in Sec. 2.5. With this information, it might be possible to identify a source region as either a known civil emitter or as a known test site, indicating a potential nuclear explosion.

The according flag has not yet been implemented, but is envisaged in the discussed categorisation concept. Flag 16 would be raised if a known civil emitter region were identified as source region and would lead to downgrading where appropriate. As of today, most civil emissions are not publicly available. A more open information policy from the facility operator side would be highly desirable.

SOH information are another valuable help to evaluate a sample as it can give important information on the sample reliability and the possible need to further review single samples. With the definitions made in Sec. 2.2.2, the SOH flag can be GREEN or YELLOW. Samples raising a RED SOH flag are screened out based on the in Sec. 3.1 defined preconditions, which are deduced themselves from the SOH criteria.

3.7 Categorisation levels

Table 3.5 and Fig. 3.2 summarise the previously discussed flags and according minimum levels. The rank order (Flag 1-4), the Xe-133m/Xe-133 ratio (Flag 15), the SRS fields (Flag 16) and SOH information (Flag 17) are not used for categorisation but only provided as additional information that shall help to assess the spectrum. The rest of the flags is used for categorisation. If one of the four relevant isotopes is detected (Flag 5-8), the minimum level for that sample is Level 2. The same is true for the metastable isotope Xe-131m being at abnormal concentration (Flag 9), as it is the less significant of the four xenon isotopes and carries a higher risk of a memory effect [42]. However, if for one of the other three xenon isotopes an abnormal concentration is measured (Flag 10-12), the spectrum is categorised at least as Level 3. If one of the two ratios Xe-133m/Xe-131m and Xe-135/Xe-133 is above the threshold (Flag 13 and 14), the sample is categorised as Level 4, if both are above the threshold as Level 5.

As can be seen from Fig. 2.11, the stable isotopic ratio (Xe-135/Xe-133) is over the suggested threshold only few days after the time of the explosion. This time is often already exceeded before the radioactivity is released, see Fig. 2.12. The metastable ratio (Xe-133m/Xe-131m) on the other hand can still be indicative of a nuclear explosion even after several days. Therefore, Level 4 categorisations are expected to come from a significant metastable ratio rather than from stable isotopes. As the highest categorisation levels refer to ratios, the algorithm consequently bases mainly on the isotopes Xe-133m and Xe-131m and not on the isotope Xe-133, which is widely accepted as the most important.

3.8 Results

In the course of this work, all noble gas spectra data available at the IDC acquired between June 2007 and June 2010 haven been analysed to test the above described algorithm. As said, not all spectra could be categorised, but preconditions were introduced to get a set of reliable data which provide the basis for statistical calculations used to compute the abnormal concentrations. Table 3.6 summarises all varied parameters and also includes the final parameter values used for the categorisation. The parameters $V_{\text{Xe},\text{min}}$, $t_{\text{c},\text{min}}$, $t_{\text{c},\text{max}}$, $t_{\text{a},\text{min}}$, $t_{\text{a},\text{max}}$, $\mu_{\text{Xe-133},\text{min}}$ and $\mu_{\text{Xe-133},\text{max}}$, which are used as preconditions for the categorisation, are chosen from the SOH characterisation information [14, 13], λ_1 , λ_2 , λ_3 , λ_4 , T_1 , T_2 and T_3 , which are used for the categorisation itself, from the categorisation concept [40] developed at the IDC. The *MDC* for Xe-135, which is also used for categorisation, and the according minimum and maximum thresholds $\mu_{\text{Xe-135},\text{min}}$ and $\mu_{\text{Xe-135},\text{max}}$ have been introduced in this work. The thresholds for the two ratios T_1 and T_2 are set at fixed values to allow a proof of concept as done in this work, while a final definition should make use of another line as already discussed by Kalinowski *et al.* [8]. With the definition applied here, nuclear explosions might be screened out, especially if the signal reaches the station only days after the event.

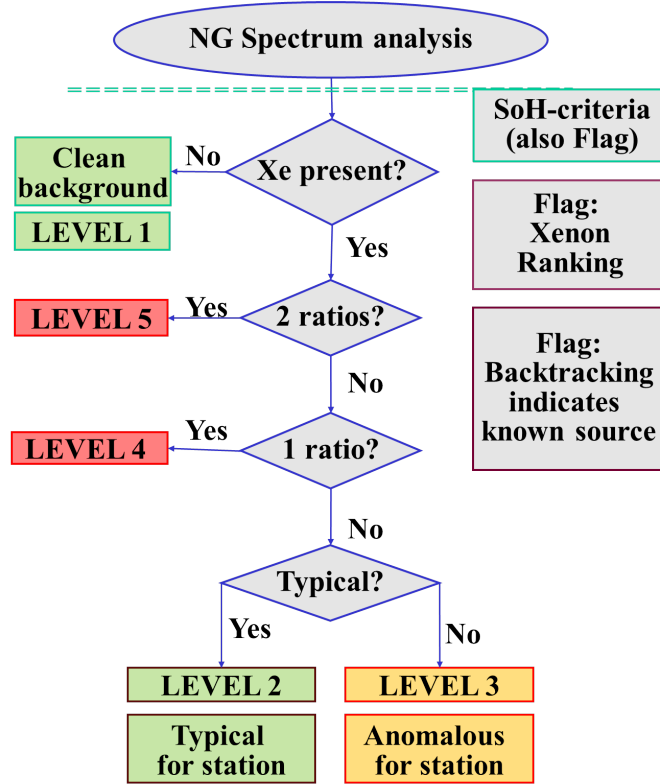


Figure 3.2: Categorisation concept as applied for the proposed algorithm. [10]
A similar categorisation concept was presented in Ref. [43].

Table 3.6: Parameters used to adapt the categorisation concept and the algorithm.

	parameter	unit	final value
$V_{\text{Xe,min}}$	xenon volume	ml	0.87
$t_{c,\text{min}}$	minimum Collection Time	h	12/6
$t_{c,\text{max}}$	maximum Collection Time	h	12/6
$t_{a,\text{min}}$	minimum Acquisition Time	h	24/48
$t_{a,\text{max}}$	maximum Acquisition Time	h	24/48
$\mu_{\text{Xe-133,min}}$	Xe-133 minimum MDC	$\frac{mBq}{m^3}$	0.001
$\mu_{\text{Xe-133,max}}$	Xe-133 maximum MDC	$\frac{mBq}{m^3}$	5
$\mu_{\text{Xe-135,min}}$	Xe-135 minimum MDC	$\frac{mBq}{m^3}$	0.001
$\mu_{\text{Xe-135,max}}$	Xe-135 maximum MDC	$\frac{mBq}{m^3}$	10
λ_1	Moving Average	days	365
λ_2	Abnormal Concentration Factor		3
λ_3	Bayes +		0.025
λ_4	Bayes -		0.975
T_1	Xe-133m/Xe-131m threshold		0.3
T_2	Xe-135/Xe-133 threshold		5.0
T_3	Xe-133/Xe-133m threshold		2.0

Table 3.7: Overall results from the automatic analysis of 25,726 noble gas spectra acquired by all IMS stations between June 2007 and June 2010.

		not cat.	Level 1	Level 2	Level 3	Level 4	Level 5
Automatic	total	4,843	7,243	12,173	1,366	60	1
	percentage	-	34.80 %	58.40 %	6.60 %	0.29 %	0.01 %
Reviewed	total					1	0
	percentage					0.01%	0%

20,843 spectra have been analysed and only 60 and 1 characterised as Level 4 and 5, respectively. By human review, these numbers could be reduced to only 1 and 0, respectively. However, another 4,843 spectra could not be categorised at this state.

The Xe-133m/Xe-131m ratio might be moved to smaller values by a memory effect due to the relatively long half-life of Xe-131m, resulting in a high background and a small Xe-133m/Xe-131m ratio. This has been observed in the aftermath of the 2006 Democratic Peoples Republic of Korea nuclear test by Ringbom *et al.* [42]. This issue is alleviated by using the Xe-133m/Xe-133 ratio as additional flag, which can help to assess a spectrum.

Table 3.7 shows the results of the final categorisation with the set of parameters as presented in Tab. 3.6. All in all, 25,726 spectra were analysed, taken at 21 different radionuclide stations. The latter are distributed all over the world, using SAUNA, SPALAX and ARIX detectors and have low as well as medium and high background xenon concentrations. 4,883 spectra did not pass the preconditions and could therefore not automatically be categorised but need further human investigation.

Out of the remaining 20,843 spectra, only one (0.01%) is categorised as Level 5 and only 60 (0.29%) as Level 4 cases. These spectra were reviewed by the standard process of an analyst within one hour, whereby the numbers could be reduced to no Level 5 and one Level 4 case. Another 1,366 (6.6%) spectra are graded as Level 3, while more than half of the samples rest within Level 2 (12,173 samples, 58.4%) and the second biggest share within the Level 1 cases (7,243 spectra, 34.8%). These are the spectra acquired throughout three complete years. If the algorithm were implemented on an ongoing basis, the absolute numbers of high categorised samples would be accordingly lower.

The presented work proves that the categorisation with xenon ratios can be used for fully automatic analysis of 81% of the unreviewed raw data even if only two relevant isotopes have been detected. Using the MDC as substitute has been proposed by Kalinowski *et al.* [8], but was never tested with a comparable high number of samples. The small number of samples categorised as Level 4 and Level 5 can be easily and efficiently assessed by human analysts with higher priority. In a next step the other spectra can be reviewed, again starting with the then highest level, which would be Level 3. Automated processing can facilitate and speed up the analysis of noble gas spectra and therefore help to guarantee an effective verification of the Comprehensive

Nuclear-Test-Ban Treaty.

4 Detectability of historic tests

In this section the previously validated five level categorisation concept is applied to historical nuclear tests, whose emissions propagation is simulated with ATM. This way, the capability to hypothetically detect historical tests conducted at the NTS with today's IMS network using the developed categorisation algorithm is determined. Therefore, the nuclear tests are transferred from the year they were originally conducted to the period between 17.02.2008 and 16.02.2009. This period was chosen because it provides the best data availability of actual IMS measurements at the used stations [36]. The actual measurements supply a realistic background for the hypothetical test emissions. The nuclear tests were originally conducted between 16.12.1964 and 08.12.1989. From all tests reported by Schoengold *et al.* [33] and edited by Martin Kalinowski [9], all those 92 releases were selected, where at least three of the four relevant xenon isotopes are reported. Two releases, for which no real IMS measurements are available are not further regarded. The missing xenon isotope Xe-131m is deduced from the measured xenon activity concentrations. The propagation of those activity concentration releases to the IMS stations is then simulated and added to the corresponding real measurements in the period from 17.02.2008 to 21.02.2009. From these overall concentrations the xenon ratios are calculated and the samples are categorised.

As this part of the work was done in Hamburg and Rome, access to the IDC databases and software was not given any more. Much less data was available and quality control more difficult. Therefore, used data as well as the applied categorisation algorithm slightly vary from those used in Sec. 3. As one consequence the focus in this section is on Level 4 and Level 5 categorisation only, the other Levels are not further differentiated.

4.1 Nuclear underground test data

Table A.1 summarises the released xenon activities for 92 of the 94 nuclear underground test releases reported by Schoengold *et al.*, where three of the four relevant xenon isotopes were measured. The Xe-131m activities have been added by the author. The given start and stop time are those after transfer into the period from 17.02.2008 to 21.02.2009 and after adjustment to the three hours intervals required by FLEXPART. The last hypothetical nuclear weapon test is conducted on January 27th 2009. The 92 releases belong to 85 nuclear tests, for seven tests two releases are reported, which means radioactivity was released at two different times. However, in this study all releases are assessed independently from each other.

Figure 4.1 shows the 92 absolute Xe-133 activity releases for nuclear underground tests conducted at the NTS as a function of time, as well as the duration of the releases (horizontal bars). The plot is analogous to Fig. 2.12. The vertical bars display the activity error. Only six unfiltered and no single uncontrolled release is included in the used dataset. All releases are distinctly delayed, at least 31.5 hours. The operational

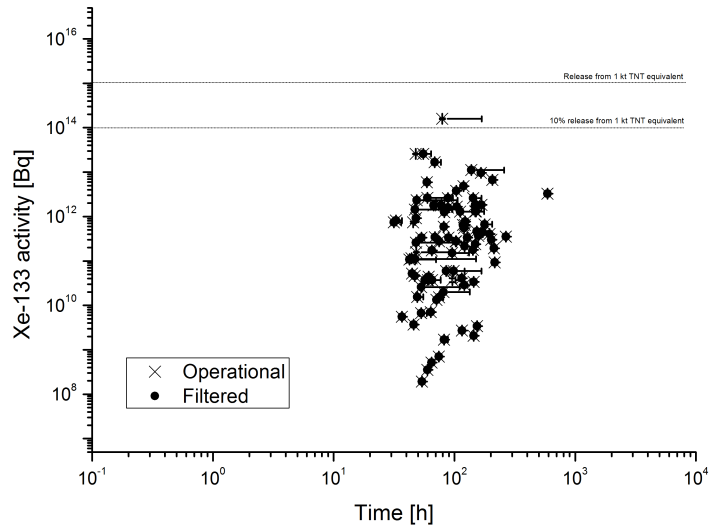


Figure 4.1: Absolute Xe-133 activities for the 92 releases at the NTS as a function of time.

The releases are differentiated in uncontrolled (circle), operational (x) and filtered (solid circle).

and mostly filtered releases are accordingly relatively small. Out of the 92 nuclear underground test releases, only one exceeds the defined quantity of 10^{14} Bq of released Xe-133 activity (release #2, $C_{\text{Xe-133}} = 1,59 \cdot 10^{14}$ Bq). The remaining 91 releases are smaller than the quantity the CTBTO IMS is designed to detect. The sums of both releases for those seven nuclear underground tests, for which two releases are reported are still below 10^{14} Bq, as can be deduced from Tab. A.1. The released activities vary over eight orders of magnitudes (smallest release: #75, $C_{\text{Xe-133}} = 2.59 \cdot 10^6$ Bq).

4.2 Estimation of Xe-131m

The isotope Xe-131m is not reported for any of the 92 releases. Therefore, the Xe-131m activity concentration has to be deduced from the other three actually measured xenon activity concentrations and their ratios, respectively. Due to radioactive decay the ratios vary over time (see Fig. 2.11) and the delay Δt between origin and release needs to be determined. This is done from the explosion time t_e , release time t_r and release duration Δt_r reported by Schoengold *et al.*:

$$\Delta t = t_r + \frac{\Delta t_r}{2} - t_e . \quad (16)$$

With Δt and the evolution of fission products simulated by Kalinowski *et al.* [8] and

Liao [44] the expected radioxenon ratios are derived. Kalinowski *et al.* also showed that there is high confidence that the airborne xenon activity ratio will exhibit negligible fractionation irrespective of the release scenario for an operational release [8]. Therefore, there is no fractionation assumed for the simulation of the ratios. As no information on the kind of nuclear weapon is available, the arithmetic mean of the xenon ratios from fission energy neutrons of uranium-235 and plutonium is used. From the simulated ratio $R_{\text{Xe-133m}/\text{Xe-131m}}$ and the measured activity concentration $C_{\text{Xe-133m}}$ the sought-after xenon concentration $C_{\text{Xe-131m}}$ is calculated:

$$C_{\text{Xe-131m}} = \frac{C_{\text{Xe-133m}}}{R_{\text{Xe-133m}/\text{Xe-131m}}} \quad (17)$$

For quality control the according measured ratio $\frac{C_{\text{Xe-135}}}{C_{\text{Xe-133}}}$ is also computed and compared to the simulated ratio $R_{\text{Xe-135}/\text{Xe-133}}$ at the respective time Δt . The input file for all NTS data including the activity concentrations of all four relevant radioxenon isotopes with errors is rendered in Tab. A.1 in the annex.

4.3 Hypothetical International Monitoring System measurements

The propagation of the four xenon activity concentrations for the next fourteen days from the release at the NTS is then simulated by multiplying them with the according SRS fields. The SRS fields are provided by Michael Schöppner, who is Ph.D. student at the University Roma Tre. He calculated the SRS fields with FLEXPART 8.2, using a backwards model (see Sec. 2.5). While the resolution can theoretically be infinite it is actually limited by computational capacity and the resolution of the input data. The meteorological fields used come from the European Centre for Medium-Range Weather Forecasts (ECMWF) and have a spatial resolution of one degree in latitude and longitude respectively and a time resolution of three hours. The hypothetical nuclear test input data is accordingly chosen to have the same resolution in space and time, which also reflects itself in the calculated SRS fields.

The IMS stations in northern America and Europe are most likely to detect a signal from the NTS. This is expected because of the geographical proximity and the general wind direction towards the east in the medium latitudes of the northern hemisphere. Therefore, only the six IMS stations USX74, USX75, CAX16, CAX17, DEX33 and SEX63 are used in the simulation, as well as the radionuclide laboratory CAX05, which also serves as national noble gas station and is well situated to detect an event located at the NTS. The locations of the used stations are given in Tab. 4.1, a frequency distribution of the data availability in Fig. 4.2.

Multiplying the released activity concentrations by the SRS field gives the amount of xenon $C_{i,H}$ which would reach the stations, which is then added to the concentrations actually measured by the stations $C_{i,B}$ at the according times:

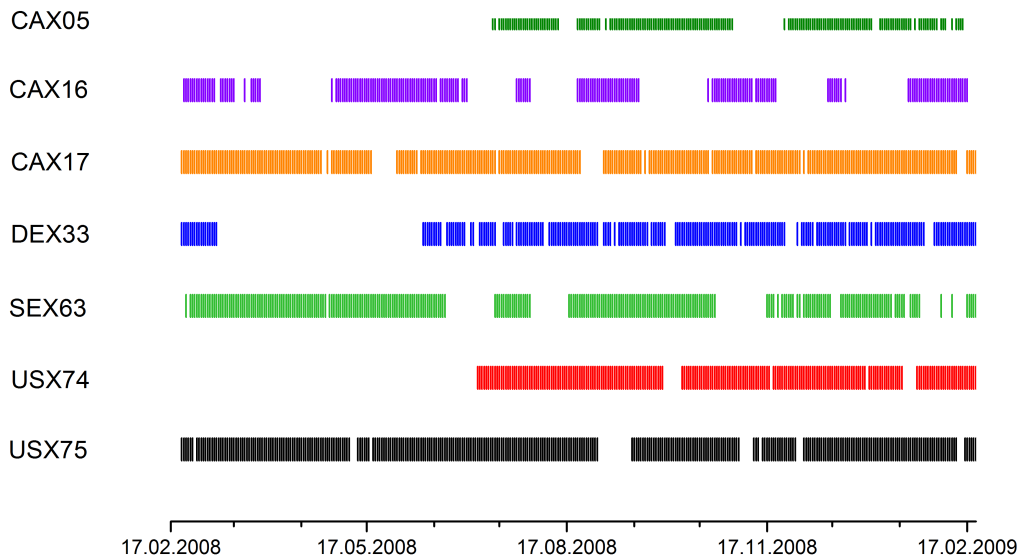


Figure 4.2: Frequency distribution of the available IMS measurements at the radionuclide laboratory CAX05 and the IMS stations CAX16, CAX17, DEX33, SEX63, USX74 and USX75 between 17.02.2008 and 21.02.2009.

Table 4.1: Locations of the NTS, where the releases occur (source) and of the seven stations, where the measurements are simulated (receptors).

Station_code	Location	Latitude [°]	Longitude [°]
-	NTS	37.0	-116.0
CAX05	Ottawa, Ontario	45.3	-75.4
CAX16	Yellowknife, NWT	62.5	-114.5
CAX17	St. John's, NL	47.6	-52.7
DEX33	Schauinsland/Freiburg	47.9	7.9
SEX63	Stockholm	59.2	17.6
USX74	Ashland, KS	37.2	-99.8
USX75	Charlottesville, VA	38.0	-78.4

Table 4.2: Preconditions as applied for the categorisation of the hypothetical nuclear tests.

	SAUNA	SPALAX
gss.status		“R”
gsd.spectral_qualifier		“FULL”
method_id		11
t_c	$6 < t_c < 24$	$12 < t_c < 48$
V_{Xe}		$> 0.87ml$
MDC for Xe-133	$0.001mBq < mdc < 5mBq$	
MDC for Xe-135	$0.001mBq < mdc < 10mBq$	

$$C_{i,H+B} = C_{i,B} + C_{i,H} , \tag{18}$$

where C are the activity concentrations, $i = \text{Xe-131m, Xe-133m, Xe-133, Xe-135}$ indicates the relevant xenon isotopes, B stands for background measurements from the IDC database and H for hypothetical nuclear test contribution. The errors are calculated analogously. From these overall concentrations, the according xenon ratios are calculated.

One drawback of this data available through vDEC is that only either the xenon concentration (with error) is given, or the MDC . It appears that the concentration (and error) was deleted if it was below the MDC and vice versa. The contribution of the hypothetical tests could only be added in those cases where the according xenon concentration was given.

4.4 Calculation of isotopic ratios

From the overall concentrations $C_{i,H+B}$, the corresponding xenon ratios are calculated as described in Sec. 3.5. The preconditions can however not be completely applied as not all therefore needed information is available. Hence, the preconditions acquisition time t_a and reporting time t_r can not be used. The other preconditions, which are status, spectral qualifier, method ID, collection time t_c , xenon volume V_{Xe} , MDC for Xe-133 and MDC for Xe-135 are used as shown in Tab. 4.2. The status is “R” for all samples as only reviewed data is available. Due to data availability the MDC s are only given, where the respective xenon activity concentration is not detected and can hence only then be used as precondition. Where available, the MDC s still serve as substitute, if the respective other concentration is detected as described in Sec. 3.5.

In order to test the slightly varied algorithm on false alarms, the ratios are calculated not only from the overall concentrations $C_{i,H+B}$ as described above, but also from the pure background concentrations $C_{i,B}$ from the IMS stations.

Table 4.3: Overall results from the automatic analysis of 6,998 datasets including reviewed actual IMS measurements between February 2008 and February 2009 and hypothetical nuclear test contributions.

	not cat.	$\frac{C_{\text{Xe-133m}}^-}{C_{\text{Xe-131m}}^+}$	$\frac{C_{\text{Xe-135}}^-}{C_{\text{Xe-133}}^+}$	$\frac{C_{\text{Xe-133m}}^-}{C_{\text{Xe-133}}^+}$
Background		0	0	1,476
Background + Hypothetical Test	2,142	0	0	1,472

Of the 6,998 datasets 2,142 could be screened out and 4,856 spectra are analysed. The categorisation of the background data does not raise false alarms. However, Flag 15 (Xe-133m/Xe-133 ratio above threshold) is raised 1,476 times. For the hypothetical nuclear tests, no single dataset is categorised as Level 4. Flag 15 is raised 1,472 times.

4.5 Results

From the available IMS measurements, the NTS data and the simulations, all in all 6,998 datasets are produced. Applying the algorithm described in Sec. 4.4, 2,142 datasets (30.61%) are screened out and the remaining 4,856 datasets (69.39%) are categorised.

Table 4.3 summarises the results of the categorisation. Accounting for the background only, no increased Xe-133m/Xe-131m and Xe-135/Xe-133 ratios occur and no dataset is categorised as Level 4 or even Level 5. As the used IMS samples are already reviewed by analysts, this can be expected bearing the results of Sec. 3 in mind, where only 1 out of the 20,843 categorised samples raises a false alarm. Still, the Xe-133m/Xe-133 flag is raised 1,476 times. This shows that the algorithm is definitely optimised only for the two other ratios used for categorisation. The Xe-133m/Xe-133 ratio on the other hand is not suitable for categorisation with this algorithm.

When the hypothetical nuclear test share is added to the IMS measurements, no single metastable ratio is above the threshold, no stable ratio and 1,472 mixed ratios. Accordingly, no Level 4 is raised and no single test is detected. What might surprise is the even smaller number of Xe-133m/Xe-133 flags compared to the background analysis. It appears that no new Xe-133m/Xe-133 ratios exceeded the threshold T_3 , but four datasets are even downgraded. This is due to the use of the *MDC* as substitute: In these four cases the Xe-133m concentrations are below the *MDC* and therefore the contribution from the hypothetical nuclear tests can not be added. Xe-133 on the other hand is detected, the hypothetical share added and therefore the ratio shifted to smaller values leading to a downgrading (no flag raised).

Figure 4.3 shows the Xe-135/Xe-133 ratio plotted against the Xe-133m/Xe-131m ratio. The ratios calculated from the actual measured xenon concentrations, which are used as background are given in red (B), those where the contribution from the hypothetical nuclear tests are included are displayed in black (H+B). The latter are not clearly shifted towards higher values of the Xe-133m/Xe-131m ratio. Therefore, no Level 4 categorisations occur. The fragmentation in two areas in respect to the Xe-135/Xe-133 ratio might be due to the substitution of non-detected isotopes through the respective

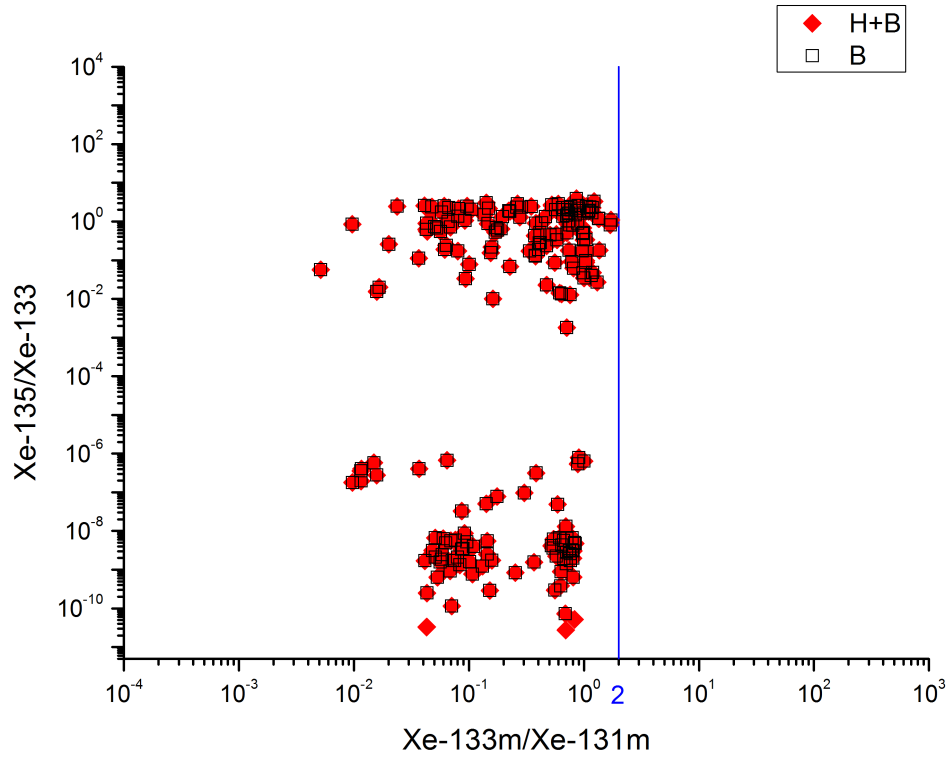


Figure 4.3: Plot of the xenon ratios $\text{Xe-135}/\text{Xe-133}$ and $\text{Xe-133m}/\text{Xe-131m}$. The ratios resulting from IMS data are given in red (B), those where the contributions from hypothetic tests are added in black (H+B). Most of the H+B entries are “hidden” behind the B entries. The plot is analogous to the plot by Kalinowski, but the y-intercept, i.e. the $\text{Xe-135}/\text{Xe-133}$ ratio are at much lower values.

Table 4.4: Assessment of the absolute contributions of the hypothetical nuclear tests at the seven stations used.

Isotope	Xe-131m	Xe-133m	Xe-133	Xe-135
$C_{i,H,max}$ [mBq]	7.54E-06	9.45E-05	4.75E-03	3.52E-06
$C_{i,H,min}$ [mBq]	0.00E+00	0.00E+00	0.00E+00	0.00E+00
μ [mBq]	3.15E-09	2.26E-08	1.62E-06	5.63E-10
σ [mBq]	1.02E-07	1.15E-06	6.06E-05	4.21E-08
$\Delta_{i,B-H,max}$ [mBq]	1.31E-05	6.36E-03	-1.66E-01	2.51E-01

$C_{i,H,max}$ is the maximal concentration contribution, $C_{i,H,min}$ the minimal non-zero contribution, μ the mean of all contributed concentrations and σ the according standard deviation. $\Delta_{i,B-H,max}$ is the maximal difference between any concentration and the according background measurement.

MDC, which leads to a distinct change in the ratio. Lower stable ratios indicate a higher delay between measurement and explosion [9], this correlation can however not be derived from the measurement data, where the background might dominate in this regard.

4.5.1 Absolute contributions of hypothetical tests

Stating that not a single of the simulated tests is categorised as Level 4 or Level 5 by the algorithm, the question arises, whether those signals could be detected using absolute concentrations. Table 4.4 assesses the absolute contributions. For the relevant four isotopes Xe-131m, Xe-133m, Xe-133 and Xe-135 are given: the maximal contributed concentration at one of the used seven stations $C_{i,H,max}$, the minimal non-zero contributed concentration at one of the used seven stations $C_{i,H,min}$, the mean of all contributed concentrations at the seven stations used μ and the according standard deviation σ and the maximal difference between any concentration and the according background measurement $\Delta_{i,B-H,max}$. The latter is defined as

$$\Delta_{i,B-H,max} = \text{Max} [C_{i,B} - C_{i,H}] . \quad (19)$$

From Tab. 4.4 can be seen, that the absolute concentration contributions are exceeding the background concentrations only for the isotope Xe-133 and only by one magnitude. They are not qualified to indicate any of the nuclear tests.

4.5.2 Source strength variation

In order to assess the potential of the categorisation algorithm the source strength is successively increased over eleven magnitudes. The results can be seen in Tab. 4.5, where f is an exponential factor and $\#_{\text{contrib}}$ the number of releases contributing elevated xenon ratios:

Table 4.5: Number of raised flags and contributing tests under variation of the source strength.

f	$\frac{C_{\text{Xe-133m}}^-}{C_{\text{Xe-131m}}^+}$	$\frac{C_{\text{Xe-135}}^-}{C_{\text{Xe-133}}^+}$	$\frac{C_{\text{Xe-133m}}^-}{C_{\text{Xe-133}}^+}$	#contrib.	$\#_{C_{\text{Xe-133}} > 10^{14}\text{Bq}}$
0	0	0	1472	0	1
1	1	0	1461	1	5
2	3	0	1416	2	27
3	24	0	1319	9	61
4	83	0	1223	27	79
5	224	0	1145	53	87
6	449	0	1094	67	91
7	719	0	1067	79	91
8	930	0	1056	83	92
9	1055	0	1056	85	92
10	1116	0	1049	86	92
11	1141	0	1032	87	92

f is the exponential amplification factor of the source strength, the following columns give the according number of alarms for the flags 13-15 and the number of releases contributing to these $\#_{\text{contrib.}}$. In addition the number of releases $\#_{C_{\text{Xe-133}} > 10^{14}\text{Bq}}$, where the absolute Xe-133 activity exceeds 10^{14}Bq , is given.

$$C_{i,\text{H}f} = 10^f \cdot C_{i,\text{H}} \tag{20}$$

All four relevant isotopes are always amplified with the same factor.

Amplification of the assumed releases at the NTS leads to higher metastable ratios and therefore more detections $\#_{\text{contrib.}}$. With increasing f , the latter rise first slowly, then faster and finally slower and slower again, apparently heading for saturation. For small amplifications only very few datasets per hypothetical nuclear test are categorised as Level 4 (i.e. have an elevated metastable ratio). The numbers might appear small, but even single Level 4's are significant, bearing in mind the results from Sec. 3, where only 0.01% of the reviewed spectra are categorised as Level 4. As expected the Level 4 categorisations are caused by the metastable ratio. Independent of the exponential amplification factor f , no single Xe-135/Xe-133 ratio is above the threshold T_2 and therefore no Level 5 cases occur. This indicates that the delay between explosion and detection was bigger than one day as the Xe-135/Xe-133 ratio strongly decreases with the chronological evolution. The mixed ratio, which is not used for categorisation even decreases with increasing f . It appears that no new Xe-133m/Xe-133 ratios exceed the threshold T_3 , but even less. This is again due to the use of the *MDC* as substitute, as described above. As the Xe-133 source strength varies for the used data set over eight orders of magnitudes (for Xe-135 even over sixteen orders of magnitudes, see Tab. A.1) it is not astonishing that some tests are detected earlier than others. However, it would be expected that these releases where the Xe-133 activity exceeds 10^{14}Bq are detected

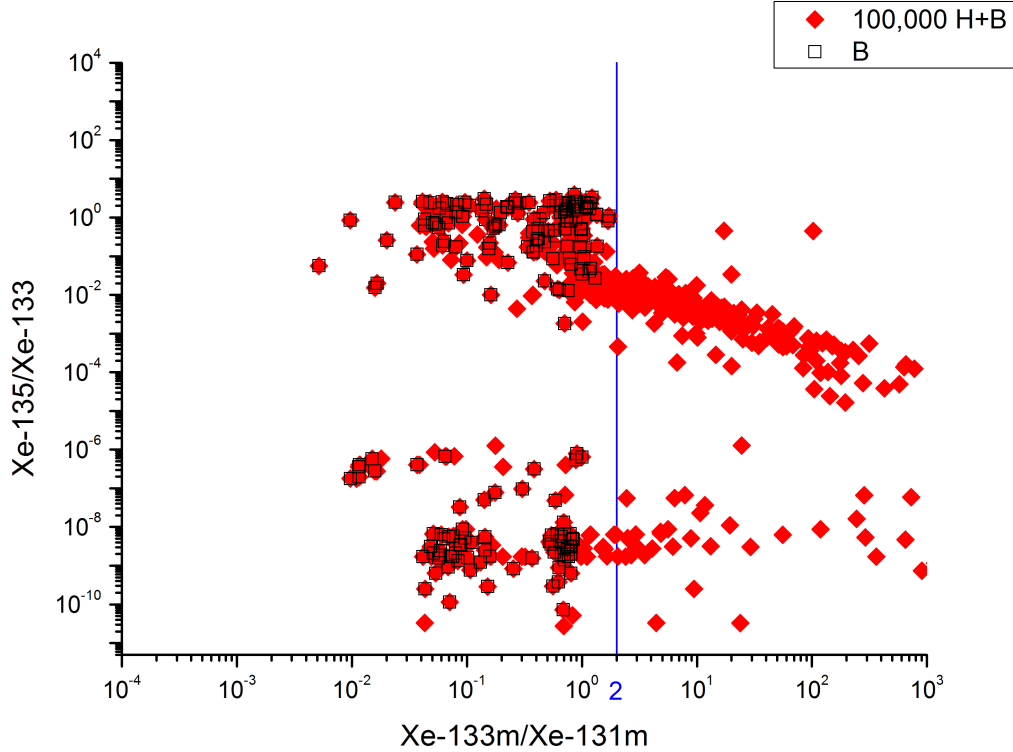


Figure 4.4: Plot of the xenon ratios $\text{Xe-135}/\text{Xe-133}$ and $\text{Xe-133m}/\text{Xe-131m}$. The ratios from the IMS data are given in red (B), those where the 100,000 times amplified contributions from hypothetical tests are added in black (100,000 H+B).

with a high probability. The last two columns in Tab. 4.5 show that this is not the case, less releases are detected.

Figure 4.4 shows an exemplary isotope plot for $f = 5$, i.e. 100,000-fold amplification. The metastable ratio is clearly shifted towards higher values with increasing source strength. This shift is leading to Level 4 categorisations, as the threshold $T_1 = 0.3$ is partially exceeded. At the same time the fragmentation in two areas in respect to the $\text{Xe-135}/\text{Xe-133}$ ratio is getting dissolved, as the background is getting less dominant.

4.5.3 Detections per station

Table 4.6 shows the number of detections (metastable xenon ratio above threshold) for the different stations, under the above introduced variation of the source strength. One has to bear in mind that the data availability is poorer for some stations than for others, e.g. for CAX05 data was available only up from July 14th 2008, see Fig. 4.2. The relative share of detections at the seven stations does not significantly change with increasing source strength. At CAX16 no releases are detected at all, independent

Table 4.6: Elevated Xe-133m/Xe-131m ratios at different exponential amplification factors of the source strength, given per station where they are measured.

f	CAX05	CAX16	CAX17	DEX33	SEX63	USX74	USX75
0	0	0	0	0	0	0	0
1	0	0	0	0	0	0	1
2	0	0	0	0	0	1	2
3	0	0	0	0	0	12	12
4	0	0	1	0	0	54	28
5	1	0	3	0	20	119	81
6	2	0	7	2	47	209	182
7	3	0	13	6	91	285	321
8	3	0	18	9	138	331	431
9	4	0	23	13	168	357	490
10	4	0	29	13	177	371	522
11	9	0	31	13	179	375	534

of the source strength. At the other stations the detections increase mostly distinctly. This can be explained with the not varied SRS-fields, which remain the same for all calculations. Some stations have more SRS entries equal to zero, which are therefore independent of source strength variation.

The assumption that the nearest stations are most likely to detect an event turned out to be only partially right. As expected, most detections occur at the two US-stations. However, the detection rates at the two European stations DEX33 and SEX63 differ significantly from each other. This might change for different times with different meteorological conditions. This speaks against simulating only part of the IMS stations and in favour of repeating the simulations with all available stations and for different times. The high dependence on the meteorological conditions makes the results at least partly random and predictions very difficult. Independently from that it is demonstrated that detections with the proposed categorisation are only possible if the released concentrations are high enough.

4.5.4 Detection thresholds

To determine the detection thresholds, the source strength of every single release is amplified by orders of magnitude until the first detection of this release with the presented algorithm (level 4 or level 5 categorisation) at one of the seven IMS stations occurs. Table 4.7 lists all releases #, the exponential amplification factor necessary to detect them f_{det} and the according Xe-133 activity $C_{\text{Xe-133,det}}$. The isotope Xe-133 has been chosen to compare the results to the 10^{14}Bq quantity defined by the United Nations

Table 4.7: Detection thresholds for the 92 releases.

#	f_{det}	$C_{\text{Xe-133,det}}$	#	f_{det}	$C_{\text{Xe-133,det}}$	#	f_{det}	$C_{\text{Xe-133,det}}$
1	3	1.85E+15	32	4	4.81E+16	63	5	3.70E+15
2	1	1.59E+15	33	7	3.70E+16	64	6	4.07E+17
3	5	3.37E+16	34	3	2.78E+14	65	6	3.26E+18
4	6	5.18E+16	35	3	2.78E+14	66	5	2.15E+16
5	3	2.59E+16	36	6	2.78E+17	67	7	5.55E+18
6	3	2.59E+16	37	8	3.70E+18	68	4	1.74E+15
7	5	7.40E+16	38	8	3.70E+18	69	5	2.89E+15
8	4	2.00E+14	39	8	4.44E+18	70	5	9.25E+15
9			40	7	5.55E+16	71	6	3.37E+16
10			41	5	1.83E+17	72	5	4.07E+15
11	4	1.11E+17	42	5	1.83E+17	73	5	6.48E+16
12	6	2.59E+16	43	5	1.67E+18	74	4	6.48E+15
13	7	5.92E+17	44	2	1.67E+14	75	10	2.59E+16
14	4	2.33E+16	45	6	3.81E+18	76	4	2.41E+15
15	7	3.70E+17	46	4	1.31E+16	77	6	1.59E+18
16	5	5.92E+17	47	4	1.31E+16	78	4	6.66E+13
17	4	1.57E+15	48	4	1.78E+15	79	7	3.40E+16
18	5	8.14E+16	49	5	6.66E+17	80	7	1.70E+16
19	6	3.00E+17	50	6	1.55E+16	81	7	5.92E+17
20	5	1.30E+17	51	5	6.66E+16	82	4	2.63E+16
21	7	1.33E+17	52	6	3.70E+17	83	11	5.18E+19
22	5	7.03E+14	53	5	4.44E+16	84	8	1.15E+19
23	4	1.92E+15	54	6	1.92E+14	85	5	9.25E+16
24	3	1.26E+15	55	3	3.44E+14	86	5	2.70E+14
25	4	7.40E+15	56	7	3.55E+18	87	9	1.52E+19
26	13	1.07E+24	57			88	9	3.55E+17
27	5	2.59E+17	58	14	4.63E+24	89	6	7.03E+14
28	7	3.33E+18	59	5	1.44E+17	90	4	1.52E+15
29	6	3.33E+17	60	5	4.63E+16	91	5	2.59E+16
30	5	1.78E+17	61	4	2.59E+16	92	7	2.07E+16
31	5	1.78E+17	62	4	5.92E+15			

gives the number of the release, f_{det} the exponential factor for which the release is detected first and $C_{\text{Xe-133,det}}$ the according hypothetical activity for the xenon-133 isotope.

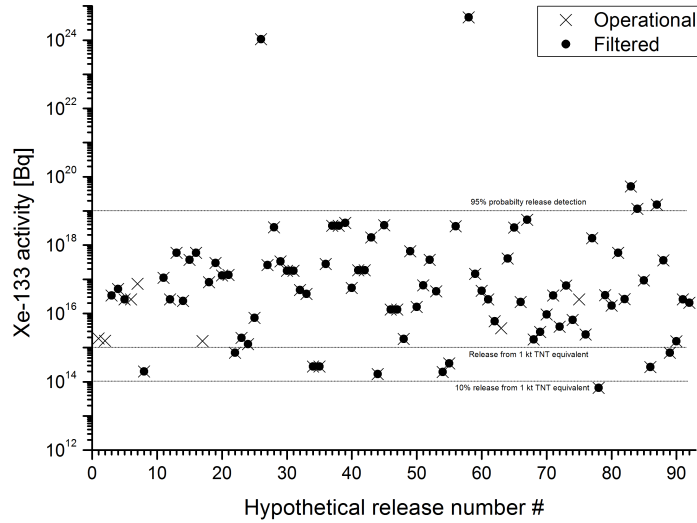


Figure 4.5: Xe-133 activities for the amplified releases.

Every release is amplified with f_{det} , which is the exponential factor for which the release is detected first. The Xe-133 activities are plotted as a function of the release number #.

General Assembly [15] and Conference of Disarmament [17], despite Xe-133m and Xe-131m are more important for the applied categorisation algorithm. Three releases (#9, #10, #57) aren't detectable, independent of the amplification. For release #9 and #10 this is probably due to few available IMS data - only 7 respectively 10 data sets can be produced. Release #57 on the other hand has a reasonable number of datasets (77), relatively high assumed activities for all four relevant isotopes and an average Xe-133m/Xe-131m ratio (see Tab. A.1). 27 of the datasets are screened out due to the high MDC-135 for the IMS-measurement. However, none of these 27 datasets would raise an alarm neither.

Figure 4.5 shows the Xe-133 activities for by f_{det} amplified hypothetical releases, where f_{det} is the exponential factor for which the release is detected first. The Xe-133 activity of one (amplified) release is below the quantity 10^{14}Bq . Another nine (amplified) releases are below 10^{15}Bq , two outliers are even above 10^{24}Bq . To reach a 95% detection probability with the applied dataset and categorisation algorithm, the significant quantity would have to be set to 10^{19}Bq (upper dashed line in Fig. 4.5).

One has to bear in mind, that only 6 of the planned 40 noble gas have been taken into account. These six stations have had longer downtimes than envisaged. In addition, only two weeks subsequent to every release have been simulated. However, Tab. 4.6 indicates, that it can not be expected to detect all releases with distinct lower amplification factors at other stations. Higher uptimes on the other hand, for example at the

IMS station USX74 might significantly improve the detection rates.

5 Conclusion and Outlook

The automatic algorithm developed in this work can categorise IMS noble gas spectra in five levels without human intervention. The algorithm's ability to categorise four fifth of the 25,726 analysed spectra with a very low false alarm rate has been demonstrated in Sec. 3. The second part of this study is the first approach to assess the detectability of historic nuclear underground test releases with the IMS. The capability to detect nuclear underground tests on the basis of xenon ratios even with only 6 out of the planned 40 IMS stations and one radionuclide laboratory within two weeks after the explosion was shown in Sec. 4. The releases could only be detected after significant amplification of the original xenon activities. However, only operational and mostly filtered releases were categorised. Prompt releases are expected to be better detectable. The CTBTO IMS is designed to detect with a probability higher than 95% any nuclear underground test releasing at least 10^{14} Bq Xe-133 activity. After according amplification of the NTS releases was still only one out of the 92 releases detected. It has been shown, that more releases are detected with higher source strengths. However, accounting for the small absolute concentration contributions puts another complexion on the share of detected releases and underlines the potential of using xenon ratios for the categorisation.

The presented algorithm has proven to be able to help analysts to prioritise those samples which are particularly significant, by categorising a huge share of the daily incoming noble gas spectra. That way, the review is facilitated and sped up which helps to guarantee an effective verification of the Comprehensive Nuclear-Test-Ban Treaty. The idea of having a five level categorisation concept was rejected in 2001 and 2011. However, this study proves the concept of using five levels for the categorisation.

The presented work remains a case study, parameter studies are needed to confirm the presented results. The distribution of the elevated xenon ratios at the stations shows the high dependence on meteorological conditions. Further studies should therefore include all available IMS stations or even determine the detection probability independently from the existing network but for a certain grid all over the world. The same is true for the source location, in this work only one single source location was simulated. Even with the achieved coverage of automatically categorised spectra being a success, the share of screened out datasets can still to be improved. Further studies could also include the Xe-133m/Xe-133 ratio in the categorisation.

Acknowledgements

Foremost I'm grateful towards my supervisor Martin B. Kalinowski and second reviewer Paul R. J. Saey. Martin Kalinowski is much more to me than the supervisor of this thesis. As head of the Carl Friedrich von Weizsäcker-Centre for Science and Peace Research he influenced my studies more than any other person. He gave me not only the opportunity to attend his lectures connecting physics to peace, but also the chance to work for him and the ZNF as student assistant. Since the very beginning Martin Kalinowski was full of interesting and innovative ideas, which kept my studies always exciting and fascinating. He is also the one who suggested me to intern at the CTBTO in Vienna. The past five years have been very fruitful for me and I'm looking forward to my future at ZNF.

I'm also very thankful to Mika Nikkinen who was my supervisor at the CTBTO and to Marco VerPELLI and Hakim Gheddou as well as all other colleagues at the IDC. All welcomed me very cordially and made my work at the IDC very interesting and exciting. I also thank Matthias Zähringer, who unfortunately left just before I came, but who still helped me a lot to understand his proposed categorisation concept.

My stay in Rome at the University Tre would not have been possible without Wolfango Plastino and Michael Schöppner. Thanks to Michael I felt home in Rome and I'm very grateful for all the time he invested to help me with the second part of this work.

Further thanks go to the operators of the used IMS stations, Clemens Schlosser, Anders Ringbom, Ted Bowyer and Kurt Ungar. All have been very cooperative. Thanks to Mark Prior (IDC) I got finally access to vDEC, too.

Malte Göttsche and Christian Hanneken gave not only feedback on my thesis draft, but are also my best friends and I do owe them for much more than only having read my draft. I can't express how important you are for me. I hope we will always stay as close friends as we are right now.

Last and most I thank my family, above all my parents for always supporting me in such comprehensiveness. You are the most important persons in my life and I love you.

References

- [1] <http://www.ctbto.org/>, accessed on May 28th, 2012. 7, 15, 16, 24
- [2] <http://ipezone.blogspot.de/2012/04/got-fission-revisiting-nukes-4.html>, accessed on May 28th, 2012. 7, 17
- [3] Lars-Erik De Geer. The xenon NCC method revisited. FOI report, October 2007. 7, 18
- [4] Lars-Erik De Geer. Radioxenon signatures from underground nuclear explosions. Poster presented at the ISS, 2009. 7, 18
- [5] Ulrich Stoelker. Radionuclide and noble gas data processing and analysis. presentation at the PTS, 2011. 7, 21, 22, 23, 26
- [6] Peder Johansson. IDC data analysis and data products. presentation at the PTS, 2011. 7, 24
- [7] Kendra M. Foltz Biegalski, Joel Rynes, and Hallie Magyar. *IDC Processing of Radionuclide Data*. IDC, idc5.2.2rev3 edition, October 2002. 7, 28, 30
- [8] Martin B. Kalinowski, Anders Axelsson, Marc Bean, Xavier Blanchard, Theodore W. Bowyer, Guy Brachet, Simon Hebel, Justin I. McIntyre, Jana Peters, Christoph Pistner, Maria Raith, Anders Ringbom, Paul J.R. Saey, Clemens Schlosser, Trevor Stocki, Thomas Taffary, and Kurt Ungar. Discrimination of nuclear explosions against civilian sources based on atmospheric xenon isotopic activity ratios. *Pure and Applied Geophysics Topical Volume*, 167:517–539, 2010. 7, 31, 40, 42, 44, 47, 48
- [9] Martin B. Kalinowski. Characterisation of prompt and delayed atmospheric radioactivity releases from underground nuclear tests at Nevada as a function of release time. *Journal of Environmental Radioactivity*, 102:824–836, 2011. 7, 32, 33, 46, 53
- [10] Frederik Postelt. The potential of radionuclide ratios for spectrum categorisation algorithms. Poster presented at the European Geosciences Union (EGU) General Assembly in Vienna, April 2011. 7, 43
- [11] A Ringbom, T Larson, A Axelsson, K Elmgren, and C Johansson. SAUNA - a system for automatic sampling, processing, and analysis of radioactive xenon. *Nuclear Instruments and Methods for Physics Research*, 508:542–553, 2003. 9, 20, 23
- [12] <http://www.nndc.bnl.gov/nudat2/>, accessed on May 28th, 2012. 9, 20
- [13] CTBTO/PTS/IDC. *SPALAX spectrum review instruction*, 0.2 edition, April 2012. 9, 29, 42

REFERENCES

- [14] CTBTO/PTS/IDC. *SAUNA/ARIX spectrum review procedure*, 0.2 edition, April 2010. 9, 29, 42
- [15] United Nations General Assembly. Resolution number 50/245. U.N. New York, U.S.A., 1996. 15, 58
- [16] O. Dahlman, S. Mykkeltveit, and H. Haak. Nuclear Test Ban - converting political visions to reality. Heidelberg: Springer, 2009. 978-1-4020-6883-6. 15
- [17] International Monitoring System Expert Group Report based on Technical Discussions held in Geneva from 6 February to 3 March 1995. Conference on Disarmament, Document CD/NTB/WP.224, 16 March 1995. 15, 58
- [18] Tibor Tóth. CTBTO Spectrum, April 2009. 17
- [19] Lars-Erik De Geer. CTBT relevant radionuclides. Technical Report PTS/IDC, April 1999. 17
- [20] K. M. Matthews. The CTBT verification significance of particulate radionuclides detected by the International Monitoring System. *NRL report*, 1:7, 2005. 17
- [21] M. Auer, T. Kumberg, H. Sartorius, B. Wernsperger, and C Schlosser. Ten years of development of equipment for measurement of atmospheric radioactive xenon for the verification of the CTBT. *Pure and Applied Geophysics*, 167:471–486, 2010. 19, 23, 32
- [22] Paul R. J. Saey. Ultra-low-level measurements of argon, krypton and radioxenon for treaty verification purposes. *ESARDA Bulletin*, 36:42–55, 2007. 19
- [23] J.-P. Fontaine, F. Pointurier, X. Blanchard, and T. Taffary. Atmospheric xenon radioactive isotope monitoring. *Journal of Environmental Radioactivity*, 72:129–135, 2004. 23, 33
- [24] Personal communication with Dr. Paul R.J. Saey. 28, 29
- [25] Lloyd Currie. Limits for qualitative detection and quantitative determination. *Analytical Chemistry*, 340:586–593, 1968. 30
- [26] K. Biegalski and S. Biegalski. Determining detection limits and Minimum Detectable Concentrations for noble gas detectors utilizing beta-gamma coincidence systems. *Journal of Radioanalytical and Nuclear Chemistry*, 248:673–682, 2001. 30
- [27] M. Zähringer, A. Becker, M. Nikkinen, P. J.R. Saey, and G. Wotawa. CTBT radioxenon monitoring for verification: today’s challenges. *Journal of Radioanalytical and Nuclear Chemistry*, 282:737–742, 2009. 31

- [28] Paul J.R. Saey. The influence of radiopharmaceutical isotope production on the global radionuclide background. *Journal of Environmental Radioactivity*, 100:396–406, 2009. 32
- [29] Paul R. J. Saey, Theodore W. Bowyer, and Anders Ringbom. Isotopic noble gas signatures released from medical isotope production facilities - simulations and measurements. *Applied Radiation and Isotopes*, 68:1846–1854, 2010. 32
- [30] Paul R. J. Saey, Clemens Schlosser, Pascal Achim, Matthias Auer, Anders Axelson, Andreas Becker, Xavier Blanchard, Guy Brachet, Luis Cella, Lars Erik De Geer, Martin B. Kalinowski, Gilbert Le Petit, Jenny Peterson, Vladimir Popov, Yury Popov, Anders Ringbom, Hartmut Sartorius, Thomas Taffary, and Matthias Zähringer. Environmental radionuclide levels in Europe: a comprehensive overview. *Pure and Applied Geophysics*, 167:499–515, 2010. 32
- [31] Paul R.J. Saey, Matthias Auer, Andreas Becker, Emmy Hoffmann, Mika Nikkinen, Anders Ringbom, Rick Tinker, Clemens Schlosser, and Michel Sonck. The influence on the radionuclide background during the temporary suspension of operations of three major medical isotope production facilities in the northern hemisphere and during the start-up of another facility in the southern hemisphere. *Journal of Environmental Radioactivity*, 101:730–738, 2010. 32
- [32] Michael Schöppner, Martin Kalinowski, Wolfango Plastino, Antonio Budano, Mario de Vincenzi, Anders Ringbom, Federico Ruggieri, and Clemens Schlosser. Impact of monthly radionuclide source time-resolution on atmospheric concentration predictions. accepted by Pageoph Topical Volume II, 2012. 32
- [33] C. Schoengold, M. DeMarre, and E. Kirkwood. Radiological effluents released from U.S. continental tests: 1961 through 1992. United States of America Department of Energy, Nevada Operations Office, 1996. 32, 46
- [34] Martin Kalinowski. Nuclear explosion time assessment based on xenon isotopic activity ratios. accepted by Applied Radiation and Isotopes, 2010. 32
- [35] Trevor J. Stocki, Guichong Li, Nathalie Japkowicz, and Kurt Ungar. Machine learning for radionuclide event classification for the Comprehensive Nuclear-Test-Ban Treaty. *Journal of Environmental Radioactivity*, 101:68–74, 2010. 32, 33
- [36] W. Plastino, R. Plenteda, G. Azzari, A. Becker, P. R. J. Saey, and G. Wotawa. Radionuclide time series and meteorological pattern analysis for CTBT event categorisation. *Pure and Applied Geophysics*, 167:559–573, 2010. 33, 34, 46
- [37] Gerhard Wotawa, Lars-Erik De Geer, Philippe Denier, Martin Kalinowski, Harri Toivonen, Real D’Amours, Franco Desiato, Jean-Pierre Issartel, Matthias Langer, Petra Seibert, Andreas Frank, Craig Sloan, and Hiromi Yamazawa. Atmospheric transport modelling in support of CTBT verification - overview and basic concepts. *Atmospheric Environment*, 37:2529–2537, 2003. 34

- [38] A. Stohl, H. Sodemann, S. Eckhardt, A. Frank, P. Seibert, and G. Wotawa. *The Lagrangian particle dispersion model FLEXPART version 8.2*. 34
- [39] A Stohl. Computation, accuracy and applications of trajectories - a review and bibliography. *Atmos. Environ*, 32:947–966, 1998. 34
- [40] Matthias Zähringer. *Xenon sample flagging and categorization concept*. CTBTO, 2 edition, February 2010. 35, 39, 42
- [41] M. Zähringer and G. Kirchner. Nuclide ratios and source identification from high-resolution gamma-ray spectra with Bayesian decision methods. *Nuclear Instruments and Methods in Physics Research Section A: Accelerators, Spectrometers, Detectors and Associated Equipment*, 594(Issue 3):400–406, September 2008. 39
- [42] A. Ringbom, K. Elmgren, K. Lindh, J. Peterson, T. Bowyer, J. Hayes, J. McIntyre, M. Panisko, and R. Williams. Measurements of radioxenon in ground level air in South Korea following the claimed nuclear test in North Korea on October 9, 2006. *Journal of Radioanalytical and Nuclear Chemistry*, 282:773–779, 2009. 42, 44
- [43] M. Nikkinen, U. Stoehlker, A. Gheddou, and M. Verpelli. Noble gas categorisation scheme. WGB 36 Presentation, 2011. 43
- [44] Yen-Yo Liao. Fraktionierung bei der Freisetzung von Leitnukliden für die Entdeckung von unterirdischen Kernwaffentests. Master’s thesis, Hamburg University, 2011. 48

A Annex

Table A.1: NTS data input file used for the simulation of the hypothetical nuclear underground tests.

#	<i>m</i>	Xe-131m [Bq]	Xe-133m [Bq]	Xe-133 [Bq]	Xe-135 [Bq]	release start	release stop
1	sg	1.34E+09	7.40E+10	1.85E+12	3.70E+10	20081219:18	20081220:06
2	sg	2.13E+11	5.18E+12	1.59E+14	8.51E+12	20080330:00	20080402:15
3	sg	1.51E+08	1.33E+10	3.37E+11	4.07E+11	20080509:21	20080510:00
4	sg	1.38E+07	1.48E+09	5.18E+10	1.04E+11	20080724:09	20080724:12
5	sg	1.39E+10	1.17E+12	2.59E+13	2.04E+13	20080823:06	20080823:09
6	sg	1.39E+10	1.17E+12	2.59E+13	2.04E+13	20080823:12	20080824:06
7	sg	3.11E+08	3.33E+10	7.40E+11	1.33E+12	20080829:12	20080829:12
8	sg	1.85E+07	5.92E+08	2.00E+10	6.29E+08	20081220:00	20081222:06
9	sg	6.31E+07	2.59E+09	1.11E+11	1.11E+10	20090115:15	20090119:21
10	sg	9.28E+08	2.26E+10	7.77E+11	5.92E+09	20090127:18	20090127:21
11	sg	3.43E+10	2.63E+11	1.11E+13	1.70E+10	20080302:09	20080307:09
12	sg	2.02E+07	1.04E+09	2.59E+10	1.44E+10	20080408:18	20080411:06
13	sg	5.54E+07	1.78E+09	5.92E+10	9.25E+08	20080418:03	20080419:15
14	sg	1.95E+09	1.07E+11	2.33E+12	6.66E+12	20080627:18	20080630:03
15	sg	2.27E+07	1.52E+09	3.70E+10	3.07E+10	20080812:21	20080813:18
16	sg	3.26E+09	2.59E+11	5.92E+12	4.44E+12	20081002:03	20081002:03
17	sg	1.18E+08	7.40E+09	1.57E+11	7.03E+10	20081107:15	20081109:15
18	sg	3.09E+08	4.07E+10	8.14E+11	3.00E+12	20080406:00	20080406:03
19	sg	8.32E+08	5.55E+09	3.00E+11	4.44E+07	20080415:03	20080415:03
20	sg	2.27E+09	4.07E+10	1.30E+12	1.96E+10	20080801:03	20080803:21
21	sg	8.85E+06	5.55E+08	1.33E+10	3.40E+09	20080813:12	20080813:12
22	sg	4.28E+06	3.03E+08	7.03E+09	3.29E+09	20080910:06	20080910:06
23	sg	5.51E+08	3.18E+09	1.92E+11	6.66E+06	20081027:12	20081027:12
24	sg	9.37E+08	4.81E+10	1.26E+12	1.70E+11	20081029:00	20081029:03
25	sg	1.73E+08	2.37E+10	7.40E+11	2.00E+12	20081207:21	20081208:00
26	sg	6.17E+07	5.18E+09	1.07E+11	1.92E+11	20090121:09	20090122:12
27	sg	1.84E+09	8.14E+10	2.59E+12	1.48E+11	20080225:09	20080225:12
28	db	2.48E+08	1.02E+10	3.33E+11	6.48E+09	20080421:18	20080421:18
29	db	4.62E+08	1.02E+10	3.33E+11	6.48E+09	20080423:06	20080423:09
30	db	1.14E+09	7.59E+10	1.78E+12	6.85E+11	20080511:09	20080511:12
31	db	1.38E+09	7.59E+10	1.78E+12	6.85E+11	20080511:06	20080511:06
32	sg	5.81E+09	1.55E+11	4.81E+12	7.77E+10	20080804:12	20080804:12
33	sg	1.81E+06	1.85E+08	3.70E+09	6.29E+09	20080817:15	20080817:15
34	db	1.75E+08	9.62E+09	2.78E+11	1.78E+10	20080909:18	20080909:18

continued on next page

ANNEX

Table A.1: Continued NTS data input file.

#	<i>m</i>	Xe-131m [Bq]	Xe-133m [Bq]	Xe-133 [Bq]	Xe-135 [Bq]	release start	release stop
35	db	3.00E+08	9.62E+09	2.78E+11	1.78E+10	20080910:06	20080910:09
36	sg	2.33E+08	8.14E+09	2.78E+11	2.41E+10	20080921:21	20080921:21
37	db	2.09E+07	1.57E+09	3.70E+10	1.65E+10	20081031:12	20081031:15
38	db	2.22E+07	1.57E+09	3.70E+10	1.65E+10	20081031:18	20081031:18
39	sg	2.66E+07	2.00E+09	4.44E+10	2.66E+10	20081125:06	20081125:06
40	sg	2.22E+06	2.81E+08	5.55E+09	1.89E+10	20080320:03	20080320:03
41	db	3.10E+09	4.44E+10	1.83E+12	1.48E+09	20080327:18	20080328:03
42	db	3.93E+09	4.44E+10	1.83E+12	1.48E+09	20080328:00	20080328:06
43	sg	9.12E+09	5.37E+11	1.67E+13	2.78E+12	20080719:12	20080719:21
44	sg	1.73E+09	5.55E+10	1.67E+12	4.44E+10	20081223:03	20081223:06
45	sg	2.66E+09	8.51E+10	3.81E+12	5.44E+10	20080303:00	20080303:03
46	db	2.07E+09	3.33E+10	1.31E+12	1.41E+09	20080702:18	20080702:18
47	db	2.32E+09	3.33E+10	1.31E+12	1.41E+09	20080702:06	20080702:09
48	sg	2.48E+08	4.44E+09	1.78E+11	1.74E+08	20081223:15	20081223:15
49	sg	1.86E+10	1.07E+11	6.66E+12	8.14E+07	20080717:03	20080717:15
50	sg	8.37E+06	7.40E+08	1.55E+10	1.92E+10	20080711:15	20080711:21
51	sg	1.74E+09	1.33E+10	6.66E+11	4.07E+07	20080225:06	20080226:09
52	sg	6.96E+08	8.88E+09	3.70E+11	2.41E+08	20080614:06	20080614:06
53	sg	9.28E+08	9.25E+09	4.44E+11	1.33E+08	20081116:21	20081117:00
54	sg	1.13E+05	9.99E+06	1.92E+08	1.07E+09	20081216:21	20081216:21
55	sg	2.30E+08	1.44E+10	3.44E+11	1.04E+11	20080326:18	20080326:18
56	sg	1.56E+09	4.07E+09	3.55E+11	9.99E+04	20080507:21	20080508:03
57	sg	2.69E+10	3.03E+11	9.62E+12	8.88E+10	20080531:12	20080531:18
58	sg	2.17E+07	2.22E+09	4.63E+10	6.29E+10	20090112:15	20090112:15
59	sg	9.43E+08	5.92E+10	1.44E+12	9.62E+11	20080316:15	20080318:18
60	sg	8.13E+08	1.17E+10	4.63E+11	8.70E+08	20080529:00	20080529:00
61	sg	4.65E+09	6.66E+10	2.59E+12	4.07E+09	20080529:12	20080530:12
62	sg	4.96E+08	2.37E+10	5.92E+11	8.51E+10	20080722:00	20080722:03
63	sg	3.90E+07	1.48E+09	3.70E+10	4.44E+09	20081106:15	20081106:21
64	sg	1.06E+09	8.14E+09	4.07E+11	6.66E+07	20080315:18	20080315:18
65	sg	8.14E+10	3.70E+09	3.26E+12	4.07E-04	20080229:03	20080229:06
66	sg	2.43E+08	5.92E+09	2.15E+11	1.30E+09	20080831:15	20080831:21
67	sg	5.17E+08	1.26E+10	5.55E+11	3.70E+08	20080410:15	20080410:15
68	sg	1.10E+08	7.77E+09	1.74E+11	7.03E+10	20080731:06	20080731:06
69	sg	3.35E+07	8.14E+08	2.89E+10	1.18E+08	20080821:15	20080821:15
70	sg	2.56E+08	1.48E+09	9.25E+10	1.11E+06	20080825:15	20080825:15
71	sg	4.61E+07	7.40E+08	3.37E+10	1.44E+07	20081003:15	20081003:15

continued on next page

ANNEX

Table A.1: Continued NTS data input file.

#	<i>m</i>	Xe-131m [Bq]	Xe-133m [Bq]	Xe-133 [Bq]	Xe-135 [Bq]	release start	release stop
72	sg	4.98E+07	1.33E+09	4.07E+10	4.44E+08	20081219:12	20081219:12
73	db	7.61E+08	2.04E+10	6.48E+11	6.66E+09	20080228:15	20080228:15
74	db	8.37E+08	2.04E+10	6.48E+11	6.66E+09	20080228:03	20080228:03
75	sg	2.15E+03	8.14E+04	2.59E+06	2.59E+04	20080320:15	20080320:15
76	sg	3.69E+08	5.92E+09	2.41E+11	3.33E+08	20081125:00	20081125:00
77	sg	1.42E+09	6.29E+10	1.59E+12	1.92E+11	20080303:06	20080303:09
78	sg	3.09E+06	2.59E+08	6.66E+09	4.07E+09	20081219:03	20081219:09
79	sg	5.16E+06	7.40E+07	3.40E+09	2.96E+06	20080502:03	20080502:03
80	sg	1.55E+06	7.40E+07	1.70E+09	2.22E+08	20080802:06	20080802:12
81	sg	8.18E+07	1.63E+09	5.92E+10	2.44E+08	20080927:18	20080930:15
82	sg	1.68E+09	9.25E+10	2.63E+12	1.55E+11	20081213:03	20081214:15
83	sg	3.23E+05	2.29E+07	5.18E+08	2.63E+08	20080425:06	20080425:06
84	sg	5.06E+07	5.18E+09	1.15E+11	1.41E+11	20080507:12	20080507:15
85	sg	4.55E+08	4.44E+10	9.25E+11	9.25E+11	20080805:15	20080805:15
86	sg	3.18E+06	8.51E+07	2.70E+09	3.33E+07	20081221:15	20081221:15
87	sg	1.14E+07	6.29E+08	1.52E+10	3.63E+09	20080505:15	20080505:21
88	sg	1.96E+05	1.55E+07	3.55E+08	1.92E+08	20080916:03	20080916:03
89	sg	4.91E+05	2.89E+07	7.03E+08	1.70E+08	20081026:18	20081026:18
90	sg	3.28E+08	9.62E+09	1.52E+11	2.70E+09	20080903:18	20080905:06
91	sg	2.32E+08	1.11E+10	2.59E+11	9.25E+10	20080226:15	20080301:15
92	sg	3.23E+06	5.18E+07	2.07E+09	2.22E+06	20081214:18	20081214:18

end

For every nuclear underground test release is given: its number #, the multiplicity *m*. (sg for single and db for double releases), the deduced Xe-131m activity concentration in Becquerel, the by Schoengold reported activity concentrations Xe-133m, Xe-133 and Xe-135 in Becquerel and the release start and stop times (yyyymmdd:hh) after transfer in the period from 17.02.2008 to 21.02.2009 and adjustment to the three hours intervals required by FLEXPART.